Journal of South American Earth Sciences 70 (2016) 279–297

Contents lists available at ScienceDirect

Journal of South American Earth Sciences

journal homepage: www.elsevier.com/locate/jsames

Magnetic properties of the remagnetized Middle-Ordovician limestones of the Ponón Trehué Formation (San Rafael Block, central-western Argentina): Insights into the Permian widespread Sanrafaelic overprint

Sabrina Y. Fazzito [a, b, *], Augusto E. Rapalini [a, b]

[a] Laboratorio de Paleomagnetismo Daniel A. Valencio, Instituto de Geociencias Básicas, Aplicadas y Ambientales de Buenos Aires (IGEBA), Departamento de Ciencias Geológicas, Facultad de Ciencias Exactas y Naturales, Universidad de Buenos Aires, Intendente Güiraldes 2160, Pabellón II, Ciudad Universitaria, C1428EGA, Buenos Aires, Argentina

[b] Consejo Nacional de Investigaciones Científicas y Técnicas (CONICET), Argentina

ARTICLE INFO

Article history:
Received 11 December 2015
Received in revised form
27 April 2016
Accepted 26 May 2016
Available online 30 May 2016

Keywords:
Remagnetized carbonates
Magnetic properties
Magnetic fabrics
Sanrafaelic remagnetization
San Rafael Block
Mendoza province
Cuyania

ABSTRACT

The widespread Sanrafaelic remagnetization reset most of the early Cambrian to mid-Ordovician carbonate platform of the Argentine Precordillera and the calcareous units of the San Rafael Block. We conducted a detailed rock-magnetic study on the Middle-Ordovician limestones of the Ponón Trehué Formation at both limbs of a tight anticline exposed in the San Rafael Block (Mendoza province, central-western Argentina) that are carriers of a syntectonic magnetization of Permian age. We found that the magnetic overprint in the Ponón Trehué Formation is carried by both pyrrhotite and magnetite, with goethite and subordinate haematite likely related to weathering. Hysteresis parameters, frequency dependence of magnetic susceptibility, Cisowski and modified Lowrie-Fuller tests suggest the presence of ultrafine particles of chemical origin. Demagnetization of natural remanent magnetization and of three-axis isothermal remanence confirm pyrrhotite and magnetite as important contributors to the remanence. Both minerals carry the same magnetic syntectonic component suggesting a coeval or nearly coeval remanence acquisition and therefore mineral formation. This and the results of the magnetic fabric analyses indicate an authigenic origin of the magnetic minerals during folding associated with the Sanrafaelic tectonic phase (ca. 280 Ma). Although the chemically active (oxidizing?) fluids expelled from the orogen as it developed in the early Permian is a viable explanation for the Sanrafaelic remagnetization, the role of the nearly coeval magmatism in Precordillera and the San Rafael Block remains to be properly evaluated.

1. Introduction

The significance of studying episodic widespread remagnetizations not only concerns the limitation that regional overprinting of primary magnetizations imposes on the availability of good quality palaeomagnetic poles for palaeogeographic reconstructions, but also in the evaluation of large-scale tectonic events and the related physical and chemical processes that originated such magnetic resetting. An especial concern exists for South America since some poorly defined intervals of the APWP give rise to controversies about its palaeogeographic evolution whereas detailed rock-magnetic studies of some of the main regional remagnetization phenomena are still lacking (for a recent review of these, see Font et al., 2012).

The case of the regional Sanrafaelic Permian overprint is particularly interesting because it is responsible for the failure of getting primary magnetizations from most Lower to Middle Palaeozoic rocks of the Argentine Precordillera (mostly from the Cambro-Ordovician carbonate platform) and the San Rafael Block. Both areas are part of Cuyania (Fig. 1, see Ramos, 2004 and

* Corresponding author. Laboratorio de Paleomagnetismo Daniel A. Valencio, Instituto de Geociencias Básicas, Aplicadas y Ambientales de Buenos Aires (IGEBA), Departamento de Ciencias Geológicas, Facultad de Ciencias Exactas y Naturales, Universidad de Buenos Aires, Intendente Güiraldes 2160, Pabellón II, Ciudad Universitaria, C1428EGA, Buenos Aires, Argentina.

E-mail addresses: sabrinafazzito@gl.fcen.uba.ar (S.Y. Fazzito), rapalini@gl.fcen.uba.ar (A.E. Rapalini).

http://dx.doi.org/10.1016/j.jsames.2016.05.012
0895-9811/

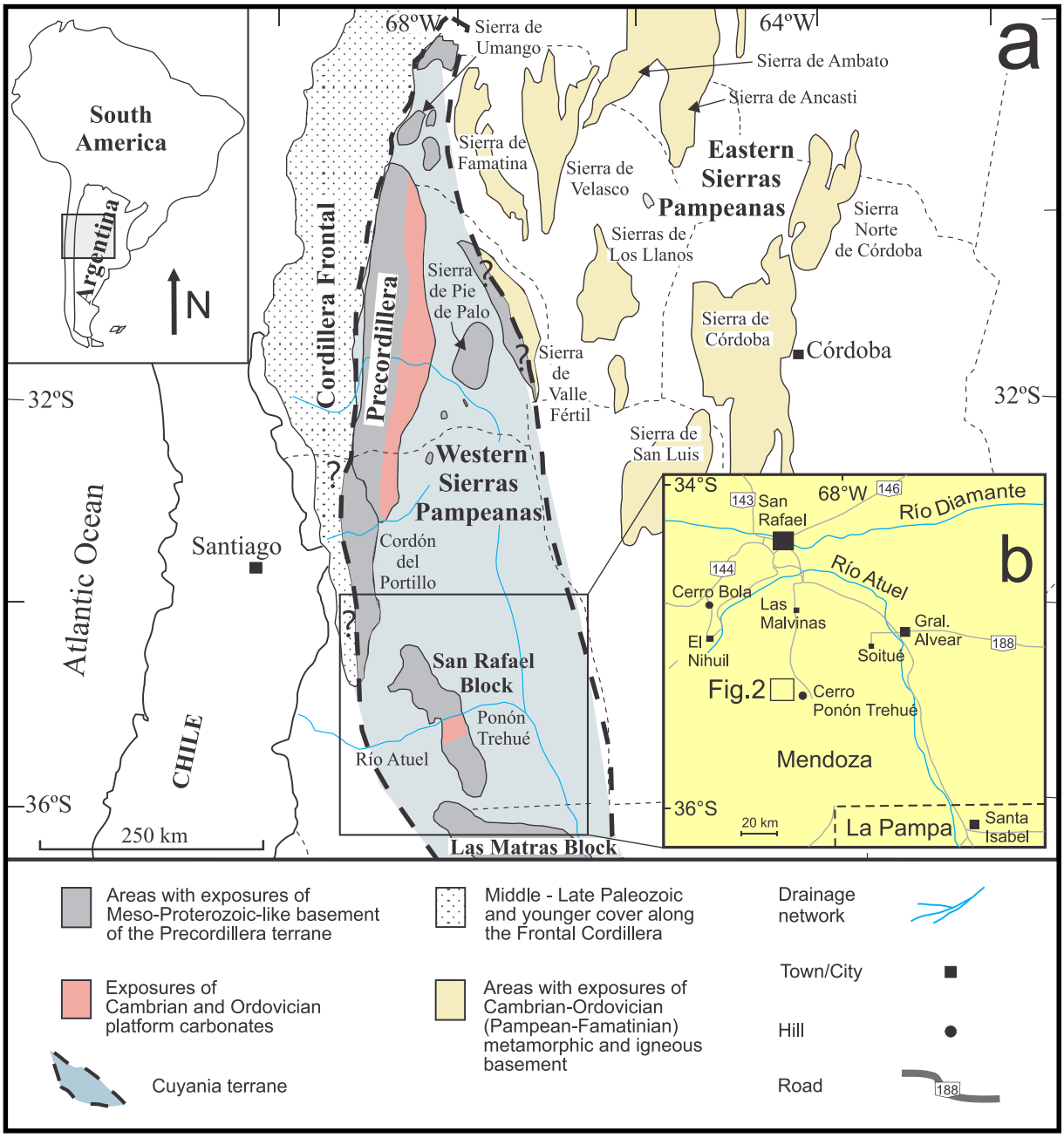

Fig. 1. a) Map of the main morphotectonic units in central western Argentina. b) Detail of the San Rafael Block modified from Cuerda and Cingolani (1998) and Astini (2002). The Ponón Trehué area (Fig. 2) is indicated.

references therein), which is interpreted as an exotic terrane derived from Laurentia and accreted to Gondwana in the middle to late Ordovician (Astini et al., 1995). Palaeomagnetic evidence for such origin has been reduced to the palaeomagnetic pole from early Cambrian red clastic sediments of the Cerro Totora Formation (Rapalini and Astini, 1998; Rapalini, 2012), plus the palaeomagnetic pole from the early Caradoc clastic sedimentary rocks of Pavón Formation exposed in the San Rafael Block (Rapalini and Cingolani, 2004). None of them have been affected by the broad remagnetization that took place during the Sanrafaelic orogeny (Kleiman and Japas, 2009 and references therein). Among the cases that were ascribed to the Sanrafaelic overprint there are: i) in the Western Precordillera, the early Permian syntectonic remagnetizations of the late Carboniferous clastic sediments of the Hoyada Verde Formation (Bobbio et al., 1990) and the igneous rocks of the late Ordovician Alcaparrosa Formation (Vilas and Valencio, 1978; reinterpreted by Rapalini and Tarling, 1993), although the latter has been disputed by Geuna and Escosteguy (2006), ii) in the Central Precordillera, the late early Permian postectonic remagnetization of the early Ordovician San Juan Formation (Rapalini and Tarling, 1993), iii) in the Eastern Precordillera, the late Permian postectonic remagnetization of the late Cambrian-early Ordovician La Flecha, La Silla and San Juan Formations (Rapalini et al., 2000), iv) in the Northern Precordillera, the late Permian pretectonic remagnetization of the late Cambrian La Flecha Formation (Rapalini and Astini, 2005), and v) the early Permian syntectonic remagnetization of the limestones of the Middle-Ordovician Ponón Trehué Formation in the San Rafael Block (Truco and Rapalini, 1996). The

Sanrafaelic remagnetization seems to show a migration of a pervasive remagnetizing front in which the geologic units in the Western Precordillera were affected during the early Permian while those in the Eastern Precordillera were remagnetized during the late Permian. This has been interpreted as possibly caused by an eastward migration of fluids expelled from the orogenic area (Rapalini and Astini, 2005). On the other hand, there is a lithological control evidenced by the primary magnetization found in some units, i.e. the red beds of the Cambrian Cerro Totora Formation, in the northern areas of the Precordillera (Rapalini and Astini, 1998), and the clastic sediments of the Pavón Formation in the San Rafael Block (Rapalini and Cingolani, 2004). To achieve a full comprehension of the chemical and physical processes that took place during the Sanrafaelic orogeny, and therefore its origin, detailed and systematic rock-magnetic studies are needed.

In this work we report a detailed rock-magnetic study on the Middle-Ordovician limestones from the Ponón Trehué Formation (San Rafael Block, Mendoza province, central-western Argentina, Fig. 1) from which Truco and Rapalini (1996) obtained a late Palaeozoic syntectonic palaeomagnetic pole (PT: 53.9°S, 25.4°E, dp = 6.2°, dm = 9.9°, N = 6). Stepwise tectonic correction indicated that this unit acquired an early Permian magnetization during 21% of folding. Previous poles from other units exposed in the Argentine Precordillera, which were also remagnetized during the early Permian as a consequence of the Sanrafaelic tectonic phase, are consistent with the PT pole position. The PT palaeopole constituted the first evidence for a broad regional remagnetizing event occurring in the Precordillera. The present work, using the samples gathered by Truco and Rapalini (1996), tries to better understand the remagnetization event. We examine the carriers of the secondary magnetization together with the rock-magnetic properties that are considered the worldwide fingerprints of remagnetization in carbonates. A magnetic fabric study by the methods of anisotropy of magnetic susceptibility and anisotropy of anhysteretic remanence complements our investigation.

2. General geologic setting and stratigraphy

The San Rafael Block and the Argentine Precordillera integrate the composite terrane called Cuyania (Ramos, 1995, Fig. 1). Both areas have in common an early Palaeozoic carbonate platform well dated by fossil records and a Grenvillian-age basement (Astini et al., 1996; Ramos et al., 1998; Thomas et al., 2000; Ramos, 2004). The Ponón Trehué Formation, a carbonate-siliciclastic sequence, crops out in southern areas of the San Rafael Block. The oldest rocks exposed in the study area correspond to metamorphic rocks of Mesoproterozoic ages around 1.1 Ga (Cerro La Ventana Formation, Cingolani and Varela, 1999; Cingolani et al., 2005, Fig. 2) that have been correlated with coeval rocks in the Sierra de Pie de Palo (McDonough et al., 1993) and the Umango, Maz and Espinal Ranges (Abre et al., 2011, and references there in), several hundred km north. The Ordovician Ponón Trehué Formation lays unconformably on this Precambrian basement (Criado Roque and Ibañez, 1979). These rocks were first studied by Padula (1951), followed by Núñez (1979). More recent studies were presented by Bordonaro et al. (1996), Heredia (1996), Truco (1996), Truco and Rapalini (1996), Cingolani and Varela (1999), Astini (2002), Beresi and Heredia (2003), Cingolani et al. (2005), Heredia (2006), Heredia and Rosales (2006) and Abre et al. (2011). Along these decades different formal names have been assigned to these rocks (Cingolani and Varela, 1999; Abre et al., 2011). Bordonaro et al. (1996), subdivided the Ordovician outcrops of this area into two formations: i) the Ponón Trehué Formation, a 75-m thick succession of dolomites and limestones with conodonts of late Tremadoc to Arenig age; and ii) the Lindero Formation, composed of at least 70 m of limestones, calcareous sandstones, siltstones, conglomeradic sandstones and quartzites with trilobites, brachiopods, ostracods and conodonts of Llanvirn to early Caradoc age (Baldis and Blasco, 1973; Heredia, 1982, 1996). This approach was also considered by Astini (2002) and accepted here.

The small outcrops of these two units are affected by folding and thrusting. In the sampling locality, for example, the limestones of the Ponón Trehué Formation are folded in a tight anticline, bounded by two thrust faults, the axis of which plunges less than 15° towards Az. 150° (Fig. 3).

The stratigraphy of this area is completed by several Cenozoic basaltic lava flows that configure a typical landscape of mesas due to differential erosion.

3. Sampling and laboratory methods

3.1. Sampling

In the original study of Truco and Rapalini (1996), sampling in the Middle-Ordovician limestones of the Ponón Trehué Formation (Fig. 2) involved six sites (thirty-eight samples) which were collected by means of a portable gasoline-powered drill on opposite limbs of a tight anticline (35°10′25.35″S, 68°18′35.52″W; Fig. 3). Distances between these sites were: 6 m between LN2 and LN1, 2 m between LN1 and LN3 and 4 m between LN3 and LN4, LN4 and LN5, and LN5 and LN6 (see sites location in Fig. 3). Mean strike and dip (right-hand rule) of the bedding planes is 182° and 71° for the west limb and 350° and 64° for the east limb, respectively. Both magnetic and solar compasses were used for orientation of all samples whenever possible. Magnetic compass readings were adjusted for the sampling locality declination (4°E) at the time of sampling (May 1995). Differences between these methods were not greater than 2°. Specimens were sliced into typical dimensions of 25.4 mm in diameter and 22.0 mm in height.

3.2. Remanent magnetization

Palaeomagnetic results were originally presented by Truco and Rapalini (1996), and analysed by means of Zijderveld diagrams (Zijderveld, 1967) with the magnetization components defined by Principal Component Analysis (PCA; Kirschvink, 1980) using the software SuperIAPD2000 (Torsvik et al., 2000). Standard palaeomagnetic demagnetization procedures were applied to all samples. Measurements of remanent magnetization were done with a three-axis 2G Enterprises 750R cryogenic magnetometer with SQUID-DC sensors. Two samples per site were used as pilot specimens to define the most appropriate palaeomagnetic demagnetization treatment. Thermal stepwise demagnetization was carried out with a Schönstedt TSD-1 furnace. Up to 12 steps were sufficient to unblock the magnetization (50-°C steps between 100 and 500 °C, and 25-°C steps between 500 and 575 °C). However, occasionally, demagnetization steps reached 690 °C. Alternating field (AF) stepwise demagnetization was carried out with a three-axis static degausser coupled to the magnetometer. A maximum of 10 steps were usually used (5-mT steps from 5 to 20 mT, 10-mT steps from 20 to 40 mT and 20-mT steps from 40 to 120 mT) though some intermediate steps were applied to some specimens. All magnetic components were determined by at least four consecutive demagnetization steps. AF demagnetization treatment was considered the most appropriate to define the magnetic components in four out of the six sites of the Ponón Trehué Formation (LN2, LN4, LN5 and LN6), while thermal demagnetization was the best procedure for sites LN1 and LN3.

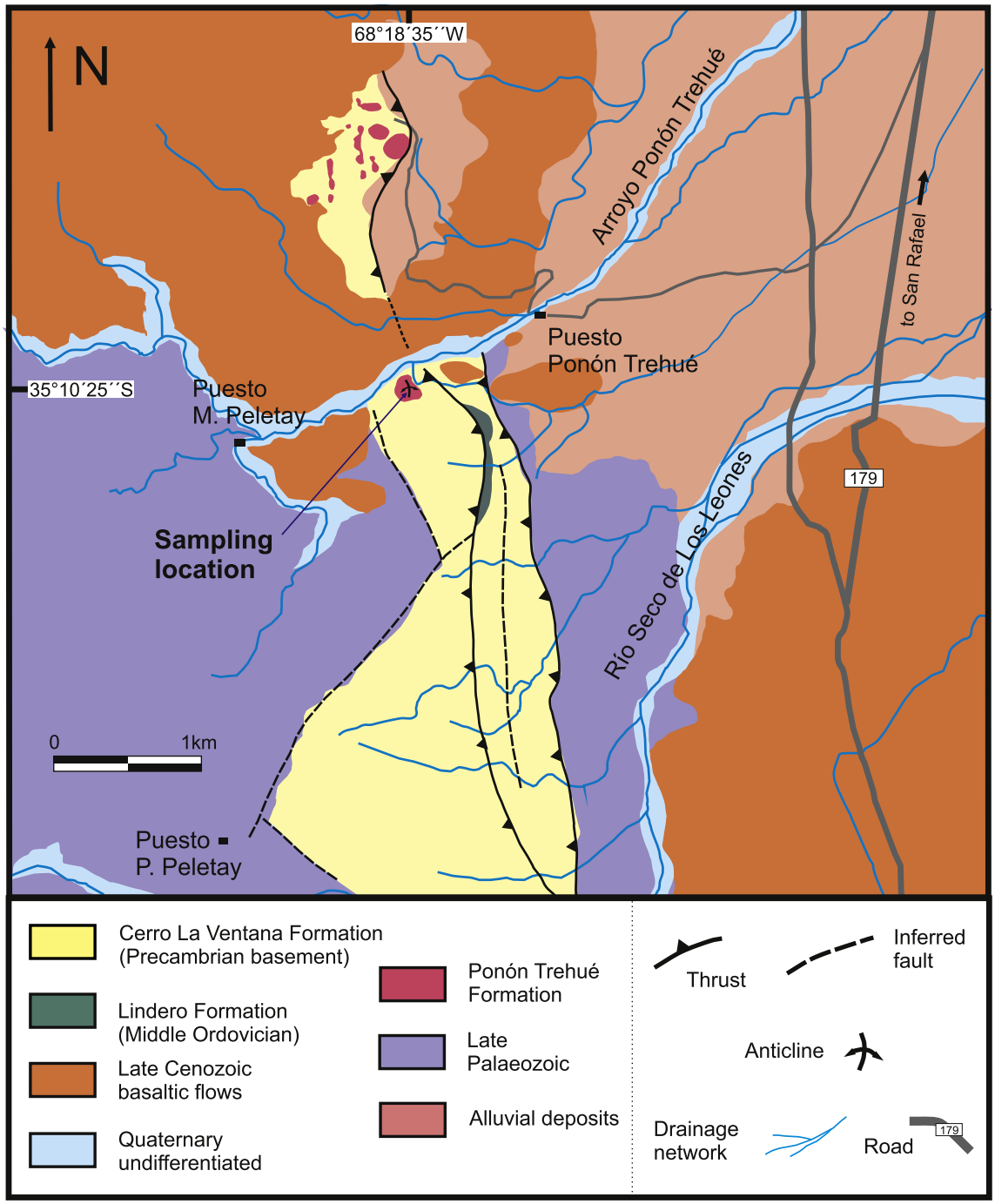

Fig. 2. Geologic map of the Ponón Trehué area (San Rafael Block) modified from Truco (1996) and Astini (2002). Palaeomagnetic sampling locality is also indicated.

3.3. Anhysteretic remanent magnetization

One sample per site was subject to stepwise acquisition of anhysteretic remanent magnetization (ARM) in a maximum alternating field (H_{ac}) of 100 mT with a direct magnetizing bias field (H_{dc}) up to 500 μT using an AGICO AMU-1 anhysteretic magnetizer. The aim was to define the range of field values in which the relationship between magnetization and direct field is linear (see results in Appendix 1). This was needed for further anisotropy studies. Remanence was measured at each step with an AGICO JR-6 spinner magnetometer.

3.4. Isothermal remanent magnetization

Stepwise isothermal remanent magnetization (IRM) was acquired with an ASC Scientific IM-10-30 pulse magnetizer between 3-mT and 2300-mT fields for one sample per site. Backfield demagnetization of IRM was subsequently applied. Magnetic remanence was measured at each step with an AGICO JR-6 spinner magnetometer. The intersection of the backfield curve with the abscissa (external applied field) was used to obtain an estimation of the coercivity of remanence (H_{cr}).

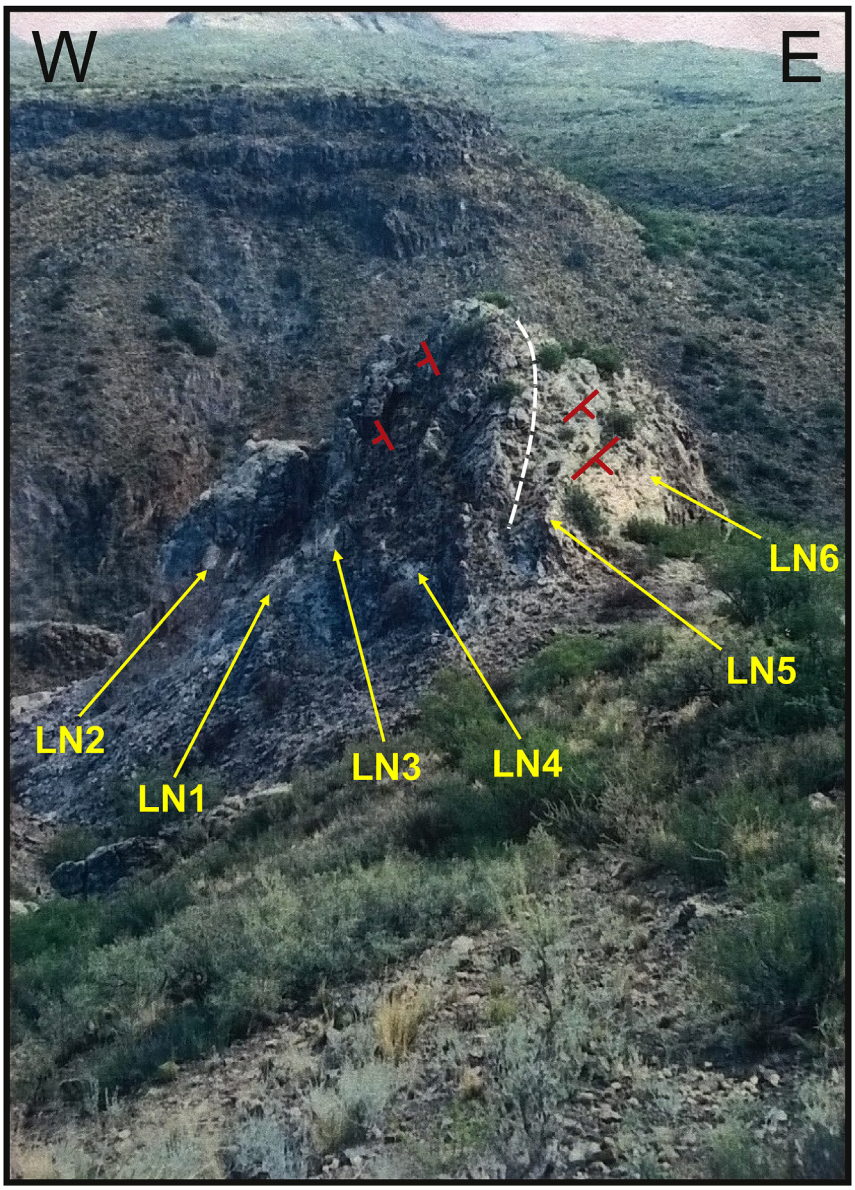

Fig. 3. The tight anticline where the Middle-Ordovician limestones of the Ponón Trehué Formation were sampled plunges less than 15° towards Az. 150°. The hinge and the bedding attitude are indicated. The six LN sampling sites are pointed out. See Fig. 2 for sampling location. Modified from Truco (1996).

3.5. Cisowski and modified Lowrie-Fuller tests

A new set of 6 samples was used to perform the Cisowski (1981) and the modified Lowrie-Fuller tests (Johnson et al., 1975). The first test is used to determine magnetic interaction degree, effective grain size and domain state (Symons and Cioppa, 2000). The second test is diagnostic of remagnetized carbonates and it is applied by comparing the stability of the ARM and IRM to the AF demagnetization. It is usually observed for remagnetized carbonates that IRM demagnetization is harder than ARM demagnetization. The ARM was acquired in a maximum AC field of 100 mT with a DC bias field of 50 μT. The stepwise AF demagnetization of ARM and IRM was carried out up to 100 mT using an AGICO LDA-3A tumbler demagnetizer.

3.6. Thermal demagnetization of tree-axis IRM

One sample per site was thermally demagnetized with an ASC Scientific TD 48 SC furnace after the acquisition of triaxial IRM in order to study the carriers of magnetization (Lowrie test; Lowrie, 1990). Samples were magnetized by a 2-T field along the z axis, a 0.4-T field along the *y* axis and a 0.1-T field along the *x* axis (representing hard, medium and soft coercivity fractions, respectively) by using the ASC Scientific IM-10-30 pulse magnetizer. Temperatures of 90 °C, 125 °C, 160 °C and steps of 50 °C between 200 °C and 500 °C and of 30 °C between 530 and 650 °C were chosen for demagnetization. Magnetization was measured with the AGICO JR-6 spinner magnetometer.

3.7. Hysteresis loops

Magnetization hysteresis loops and remanence curves were acquired for one sample per site under fields ranging −1000 to 1000 mT in a Molspin Vibrating Sample Magnetometer for each site. For magnetization curves, diamagnetic and paramagnetic effects were cancelled by subtraction of the high-field slope.

Saturation magnetization (M_s), saturation remanence (M_{rs}), remanent coercive force (H_{cr}) and coercive force (H_c) were determined from the measurements.

3.8. Thermomagnetic curves

Variation of low-field magnetic susceptibility from ambient temperature to 665 °C was measured in two samples (LN4-4C and LN5-5C) by means of an AGICO Kappabridge MFK1-FA susceptibility-meter coupled to a CS4 high-temperature furnace apparatus. Frequency was fixed at 976 Hz and peak external field at 200 Am^{-1}. The atmosphere was argon-controlled during heating to avoid oxidation.

3.9. Field and frequency variation of magnetic susceptibility

Field dependence of susceptibility was determined in two samples per site (twelve specimens) in the range 2–700 Am^{-1} at a fixed frequency of 976 Hz. Frequency dependence of bulk susceptibility was calculated on several specimens from each site by measurements at two different frequencies: f_1 (976 Hz) and f_3 (15,616 Hz) at a field amplitude of 200 Am^{-1}. The frequency dependence was quantified on selected samples (fifteen specimens) from the six sites by the parameter k_{fd} (%) = 100 × (k_{f1}-k_{f3})/k_{f1} considering correction for diamagnetic susceptibility.

3.10. Anisotropy of low-field magnetic susceptibility (AMS)

Magnetic fabrics studies of remagnetized limestones (McCabe et al., 1985; Ihmlé et al., 1989; Jackson, 1990a; Sun et al., 1993; Gialanella et al., 1994) are still scarce in the literature. Prior to carrying out destructive rock magnetic studies, the anisotropy of low-field AC magnetic susceptibility (H_{peak} = 200 Am^{-1}; f = 976 Hz) was measured in 37 specimens (six sites) with an AGICO multi-function Kappabridge susceptibility-meter (MFK1-FA) by using the spinning specimen method with rotator. Best fitting susceptibility ellipsoid was calculated on each specimen by operating the Safyr 3.2 software (AGICO) while Jelínek (1978) statistics of the AMS ellipsoids on each site was computed by using the Anisoft 4.2 software (AGICO).

The AMS axes of the diamagnetic limestones were considered taking into account their negative values (i.e. the minimum susceptibility K_3 refers to the principal susceptibility axis with the largest negative value), but the AMS scalar parameters such as *P*, *L*, *F* and *T* were defined using the absolute values of the principal susceptibilities. This convention is taken from Hrouda (2004).

3.11. Anisotropy of anhysteretic remanent magnetization (AARM)

Following the AMS measurements, the AARM was determined in 28 specimens (six sites) by the combined use of the AF demagnetizer (LDA-3A) and the anhysteretic magnetizer (AMU-1A) with support of the AREM software (AGICO) which determines the best-fit anhysteretic remanence tensor. A 100 mT-AC field (H_{ac}) and a 50 μT-DC bias field (H_{dc}, Appendix 1) were imparted according to a 12-position protocol and remanence was measured in a JR-6 spinner magnetometer. Tumble AF demagnetization was employed before each magnetization event. Remanence tensors were determined by Jelínek (1978) statistics using the Anisoft 4.2 software (AGICO).

4. Results

4.1. Palaeomagnetism

Typical demagnetization behaviours of the Ponón Trehué limestones are shown in Fig. 4a–f. Most samples showed two well defined magnetic components. Component A was isolated at low temperatures, up to 200 °C, and low magnetic fields (up to 10 mT). It is directed up and northward, close to the present-day dipole field direction, which suggests a recent origin. A viscous origin is likely for this component, although a secondary chemical magnetization carried by goethite is apparent in samples thermally demagnetized. In general, component B showed a clear trend towards the origin of the Zijderveld diagrams with unblocking temperatures around 525°-550 °C and medium destructive fields around 30–50 mT. The presence of goethite also was apparent in some specimens (LN2-1, LN4-1, LN5-2, LN6-1 and LN6-4) that were treated only by AF demagnetization as a residual remanence not erased by this procedure and coincident with Component A direction. Most sites exhibited good within-site consistency of directions of the high temperature/coercivity remanence (Component B, Table 1). Component B mean directions from both limbs of the anticline are not coincident either *in situ* or after application of full bedding corrections (Table 1, Fig. 4g and h). However, application of stepwise structural correction and McFadden (1990) fold test indicates that the remanence was acquired during folding of the anticline. Maximum value of the precision parameter κ is obtained at 21% of bedding correction, rendering a positive fold test for the partially corrected remanence (Fig. 4i). The fold test is significant at a 99% confidence level (see *k* vs. percentage of unfolding in Fig. 4j). The syntectonic nature of the remanence and the palaeopole position suggest a late Palaeozoic (Sanrafaelic) remagnetization of the studied limestones (Truco and Rapalini, 1996).

4.2. Rock magnetism

4.2.1. IRM studies and susceptibility curves

A rapid increase at low fields (<100 mT) in the IRM acquisition curves (Fig. 5) shows that a low coercivity phase is present in all samples. Sample LN3-2b saturates at ~1600 mT, revealing content of a high-coercivity mineral, possibly haematite. No saturation for the other five samples is observed at the available field range (≤2300 mT). A high-coercivity antiferromagnetic mineral phase is expected for these, like goethite and/or haematite. Backfield demagnetization of IRM confirms the broad range of coercivity phases, with values of 95 mT for LN2-5m and LN3-2b and magnitudes spanning from 225 to 585 mT for the others.

Stepwise thermal demagnetization of a three-axis IRM suggests multiple ferromagnetic mineralogy (Fig. 6). Generally, the dominant carriers of the IRM are distributed in the medium and/or hard fraction while the soft fraction gives the weakest contribution (LN1-5, LN3-3, LN5-3 and LN6-1). The soft fraction only dominates in sample LN2-5, together with the medium fraction, while in sample LN4-3 all three components provide similar contributions. The drop of the magnetization at ~90 °C of almost all coercivity fractions in all samples exhibits a clear evidence of goethite. In five out of six specimens (LN2-5, LN3-3, LN4-3, LN5-3 and LN6-1), a strong decrease in intensity between ~300 °C and 350 °C in a wide range of coercivities suggests the unblocking of pyrrhotite. High unblocking temperatures between 620 °C (LN1-5, LN3-3, LN4-3 and LN5-3) and 650 °C (LN6-1) are indicative of a contribution of haematite, not observed in sample LN2-5. Evidence for low content of magnetite was also found in all sites: all fractions of LN1-5 exhibit an important decrease in magnetization in the range

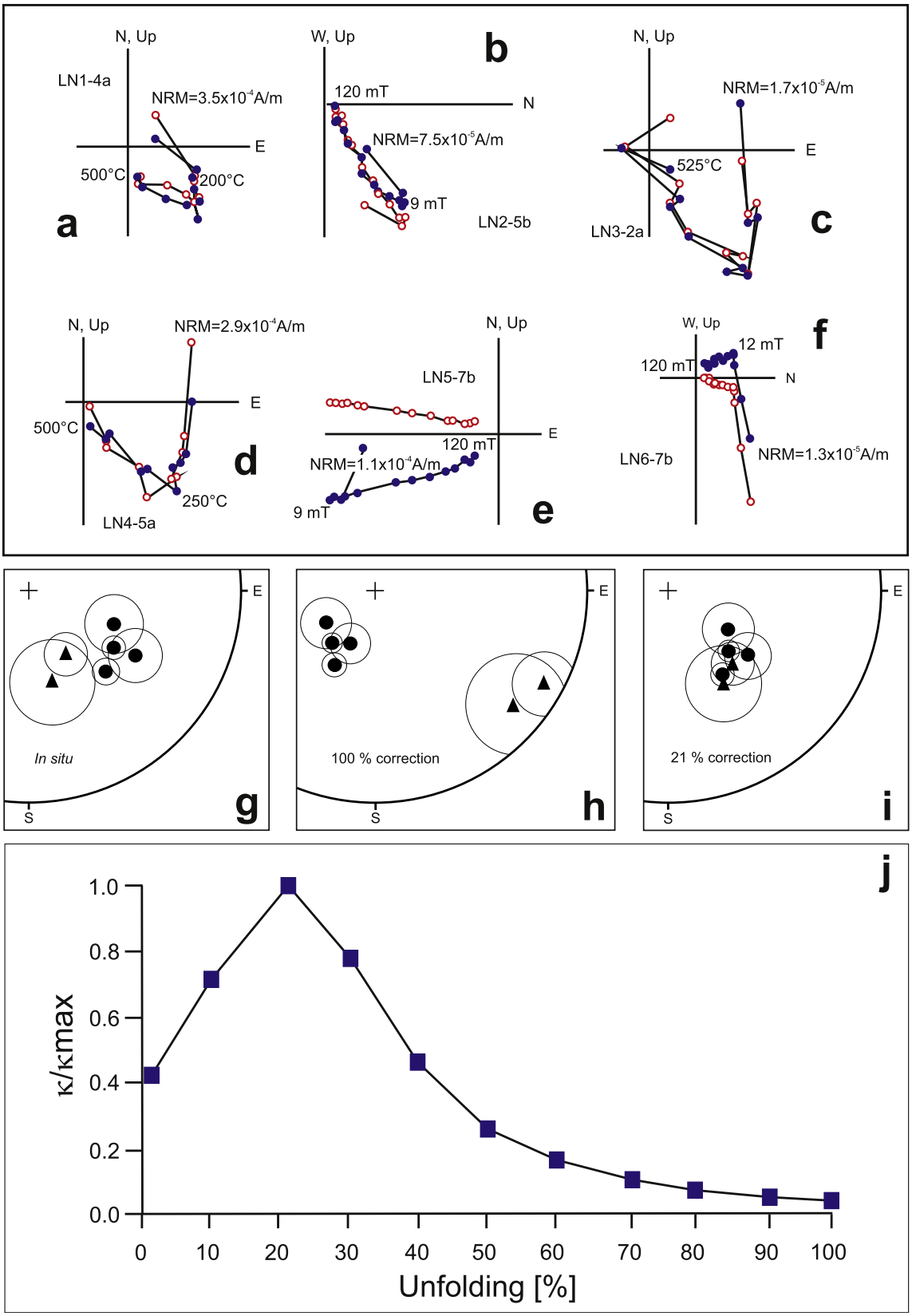

Fig. 4. a)–f) Representative Zijderveld plots (*in situ*) of samples treated by progressive alterning field (AF) or thermal demagnetization from the Ponón Trehué Formation. Open (solid) symbols indicate the projection on the vertical (horizontal) plane. Significant demagnetization steps have been indicated. NRM: natural remanent magnetization. g) *In situ* site-mean characteristic remanence directions for the Ponón Trehué Formation and their α_{95} in equal-area projection (lower hemisphere). h) Idem after 100% tilt correction. i) Idem after partial (21%) tilt correction. Circles and triangles correspond to sites on opposite limbs of the tight anticline (west and east limbs, respectively). Taken from Truco (1996). The GAD field inclination expected for the study area is −54.6°. j) Normalized κ values (precision parameter) for the mean characteristic site-mean remanence directions considering all the sampled sites *vs.* percentage of tectonic unfolding for the Ponón Trehué Formations.

Table 1
Site-mean and mean (all over the sites) characteristic remanence (ChRM) for the Ponón Trehué Formation (*in-situ*, after partial structural correction and 100% percent tilt corrected). n: number of specimens considered for calculation of the site-mean remanence; N: total number of sites used to determine the mean ChRM; Dec: declination; Inc: inclination; α_{95}: half-angle of the cone of 95% confidence about the mean; κ: precision parameter (Fisher, 1953). Taken from Truco and Rapalini (1996).

Site	n	Site-mean ChRM (Component B) *in situ*				Bedding correction		Site-mean ChRM (Component B) full corrected	
		Dec [°]	Inc [°]	α_{95} [°]	κ	Strike [°]	Dip [°]	Dec [°]	Inc [°]
LN1	6	124.8	28.2	10.0	46	182	71	205.2	58.6
LN2	3	116.8	41.5	12.2	102	182	71	234.2	59.1
LN3	5	139.2	31.7	5.2	217	182	71	208.3	45.8
LN4	6	128.0	36.0	4.6	208	182	71	217.8	54.1
LN5	6	150.5	46.9	9.5	50	350	64	120.4	6.6
LN6	5	162.4	40.3	15.8	24	350	64	130.3	11.1

Mean ChRM (all sites, in situ): N = 6 Dec: = 136.5° Inc = 39.2° α_{95} = 12.5° κ = 30.
Mean ChRM (all sites, 100% corrected): N = 6 Dec = 174.6° Inc = 49.6° α_{95} = 40.4° κ = 4.
Mean ChRM (all sites, 21% corrected): N = 6 Dec = 139.2° Inc = 44.0° α_{95} = 7.9° κ = 72.

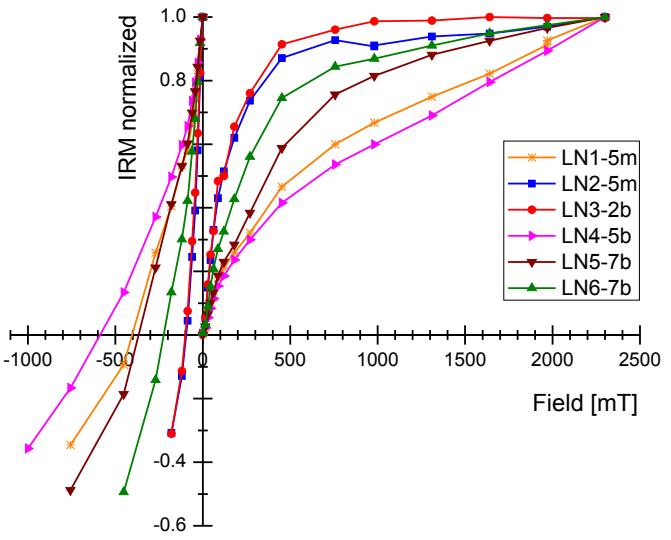

Fig. 5. Normalized isothermal remanent magnetization (IRM) acquisition curves in magnetic fields up to 2300 mT and backfield demagnetization of IRM of the limestones from the Ponón Trehué Formation.

400–530 °C, consistent with a large relative proportion of SP grains (Zegers et al., 2003, Fig. 6a); the soft fraction in LN2-5 was smoothly demagnetized to zero up to 590 °C (typical tail of MD magnetite, Dunlop and Özdemir, 2000); soft and medium fractions decrease up to zero between 400° and 560 °C in LN4-3; in LN3-3 the medium fraction gently reduces its magnetization from 530 °C (see Fig. 6c); soft and medium fractions of LN5-3 and LN6-1 reduce almost to zero at 450 °C (see Fig. 6e and f).

High-temperature thermomagnetic curves showed similar behaviours (Fig. 7). Susceptibility decrease between 60-70 °C and 120–130 °C in LN4-4c and LN5-5c corroborates the presence of goethite. Magnetic susceptibility of LN5-5c slightly falls after 300 °C suggesting pyrrhotite content in agreement with the analysis of demagnetization of three-axis IRM of specimen LN5-3 (Fig. 6e). The susceptibility of specimen LN4-4c (heating curve) starts a slight decrease between 380 and 420 °C followed by a significant increase (mineral neoformation?) and a major drop close to 550 °C, pointing to magnetite. However, how much of this has been produced during heating is not clear. The presence of large proportion of SP magnetite or titanomagnetie is consistent with unblocking temperatures between 450 °C and 550 °C observed in demagnetization of the three-axial IRM of specimen LN4-3 (Fig. 6d). A very small decrease of susceptibility between 400 and 450 °C is recognized in specimen LN5-5c, although major drop corresponds to the interval 500–550 °C suggesting the presence of magnetite. Very low amounts of haematite (T > 600 °C) are also observed in both samples. Creation of new magnetic mineral is indicated by the irreversible nature of the cooling curve, with Curie temperatures close to 550–580 °C. This points to magnetite created during thermal treatment probably by oxidation of pyrrhotite (Bina and Daly, 1994). In sample LN5-5c experimental formation of magnetite seems to continue during cooling.

Evidence of titanomagnetite or pyrrhohite content by measuring variation of bulk magnetic susceptibility against the applied AC field (Hrouda et al., 2006a, b) was not observed, probably due to the low content of ferrimagnetic grains in the limestones. This, however, can also be taken as further evidence that magnetite and not titanomagnetite is present in these limestones. At low fields (<100 Am^{-1}) the readings were noisy, so we restricted our analysis to fields greater than 200 Am^{-1}. For the twelve analysed specimens (see Appendix 2), bulk susceptibility variations were lower than 6%, so very small to non-significant variation was detected for most part of the field range.

The magnetic analysis results hitherto described are evidence of a complex magnetic mineralogy. Several methods support the presence of goethite, pyrrhotite, magnetite and minor contributions of haematite. Component A of magnetization is characterized by a direction parallel to the current GAD field with low unblocking temperatures (<200 °C) and belonging, at least in part, to a high-coercivity phase for which goethite is the best candidate as the magnetic carrier (Fig. 4). Component B of magnetization was isolated between 250° and 550 °C and it has a mean destructive field lower than 50 mT (Fig. 4). This supports that the characteristic magnetization at this unit, i.e. the Sanrafaelic remagnetization at the Ponón Trehué Formation, is likely carried by either or both pyrrhotite and magnetite. Thermal demagnetization of three-axis IRM showed that the influence of haematite is low or absent (83–91% of the total IRM was removed at ~400 °C in all samples), suggesting that its presence as remanence carrier is most likely very subordinate (Fig. 6).

4.2.2. *The magnetic fingerprint of remagnetized carbonates*

The magnetic fingerprint of remagnetized carbonates (wasp-waisted hysteresis loops, contradictory Lowrie-Fuller and Cisowski tests, anomalously high hysteresis ratios, high frequency-dependent magnetic susceptibility, etc) has been already analysed in samples with multi-mineralic content (Weil and Van der Voo, 2002; Zegers et al., 2003; Trindade et al., 2004; Zwing et al., 2005; Font et al., 2006; Oliva-Urcia and Pueyo, 2007) resulting, in some cases, in intermediate or ambiguous characteristics (Jackson and Swanson-Hysell, 2012). For instance, the magnetic fingerprint in remagnetized carbonates was found as a rule by Trindade et al. (2004) in samples from the Neoproterozoic Salitre Formation (Bahia state, Brazil), with a remanence component carried by magnetite, with or without an extra component carried by pyrrhotite or haematite. In that work, the diagnostic tests of Lowrie-Fuller (modified, Johnson et al., 1975) and Cisowski (1981) failed systematically on samples with a single magnetic component carried by pyrrhotite. Measurements on Neoproterozoic remagnetized bituminous limestones from the Cáceres region (Mato Grosso state, Brazil; Font et al., 2006) with a remanence carried by a mixture of magnetite and pyrrhotite showed consistency with the magnetic proxy for recognizing secondary magnetization in carbonates.

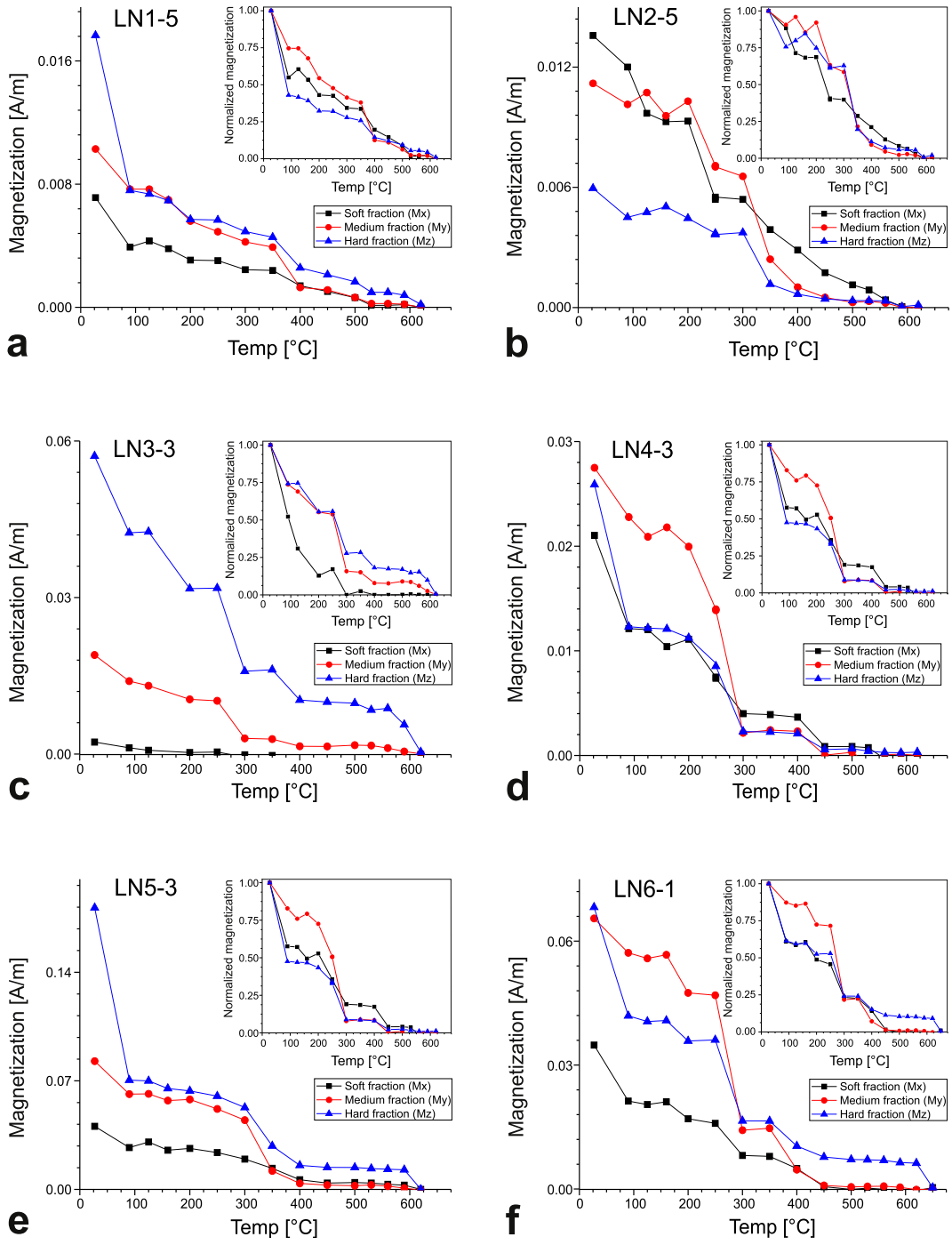

Fig. 6. Demagnetization of triorthogonal IRM (Lowrie, 1990) of specimens from the Ponón Trehué Formation. Insets: plots with normalization by coercivity fractions.

However, the diagnosis by the Lowrie-Fuller (Johnson et al., 1975) and Cisowski (1981) tests failed for samples from the Terconi quarry (Mato Grosso state, Brazil; Font et al., 2006), for which the remagnetization component is carried again only by pyrrhotite. Considering that the Sanrafaelic remagnetization in the Ponón Trehué Formation is likely carried by magnetite and pyrrhotite, and that there is haematite and goethite content in the samples, our work intends to evaluate if the typical magnetic signature of remagnetized limestones is also observed in these samples.

Very low bulk susceptibility values were measured at two frequencies on selected specimens from the Ponón Trehué Formation ($k \leq 2.6 \times 10^{-5}$ SI, Table 2). Each value is the mean value over ten successive bulk susceptibility measurements. All samples from sites LN1, LN2 and LN3 are diamagnetic. Due to the significant diamagnetic contribution in our samples, a correction was applied for calculation of frequency-dependence parameter k_{fd}. The intrinsic susceptibility of pure calcite at room temperature $(-12.09 \pm 0.50) \times 10^{-6}$SI determined by Schmidt et al. (2006) was assumed for this correction. For the most part of the samples, high k_{fd} parameters were obtained (Table 2). A mean value of 5.5% was estimated all over the sites for the corrected parameter (non-corrected values indicate a mean of 11.3%) This probably means that

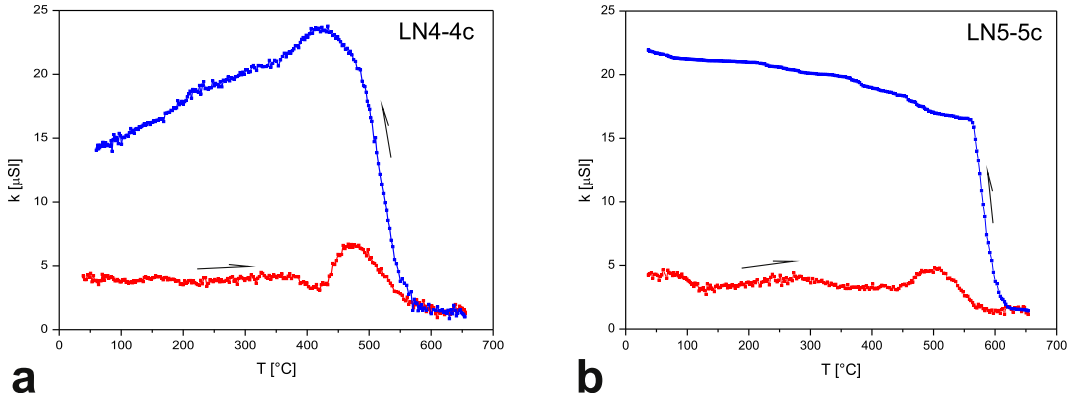

Fig. 7. High-temperature thermomagnetic curves of samples LN4-4c and LN5-5c. Arrows indicate heating (red) or cooling (blue) sense. (For interpretation of the references to colour in this figure legend, the reader is referred to the web version of this article.)

Table 2
Frequency dependence of magnetic susceptibility parameter k_{fd} in selected samples of the Ponón Trehué Formation. Values corrected by diamagnetism are indicated by kc_{fd}.

Specimen	k_{f1} [10^{-6}(SI)]	k_{f3} [10^{-6}(SI)]	k_{fd} [%]	kc_{fd} [%]
LN1-4	−2.1	−2.8	–	6.5
LN1-5	−3.5	−3.6	–	1.1
LN2-1	−4.7	−5.3	–	7.1
LN2-5b	−2.8	−3.3	–	5.8
LN3-2b	−6.2	−6.4	–	2.9
LN3-5	−3.6	−4.2	–	7.4
LN4-2	11.9	10.4	12.3	6.1
LN4-3	12.4	11.2	9.6	4.8
LN4-5b	14.1	12.4	12.0	6.4
LN5-1	8.7	6.1	25.5	10.4
LN5-5	20.3	18.3	9.7	6.1
LN5-7b	25.8	23.4	9.3	6.3
LN6-1	12.7	11.4	10.7	5.5
LN6-2b	7.1	6.7	5.5	2.0
LN6-3	1.9	17.4	7.1	4.3

there is an important contribution of a superparamagnetic (SP) fraction of ferrimagnetic grains (Dearing et al., 1996), confirming that the relatively low unblocking temperatures (525–550 °C) of the natural remanence would correspond to SP contributions (e.g. Zegers et al., 2003). Significant variation of bulk susceptibility with the frequency of the AC field is typically found for remagnetized carbonates. Strong frequency dependence was reported for remagnetized carbonates indicated by k_{fd} values usually above 5% (see examples in Jackson et al., 1993, Font et al., 2006, 2011a,b).

At high fields hysteresis loops show dominant diamagnetic (LN1-2, LN2-6, LN3-2 and LN6-6) and paramagnetic (LN4-4 and LN5-5) contributions (insets of Fig. 8). The loops were smoothed to better define their shapes and hysteresis parameters as low remanence values produced noisy curves (Fig. 8). Except for sample LN2-6, all corrected hysteresis loops are slightly wasp-waisted, i.e. the central part is narrower than the lower and upper segments (Fig. 8). These constricted hysteresis loops are typical of remagnetized carbonates all over the world (Kodama, 2012). This shape is due to the presence of mixed ensembles with contrasting coercivities as a result of the combination of two magnetic minerals or contributions of grains in different domain states (Jackson and Swanson-Hysell, 2012 and references there in). The multimineralic magnetic nature of the limestones of the Ponón Trehué Formation suggests that the first feature is the most likely explanation for the constricted loops of these rocks, although contribution of SP grains, as mentioned above, also can contribute to the hysteresis loop shape. We analysed the hysteresis ratios by means of a Day-type diagram (Day et al., 1977; Dunlop, 2002a,b, Fig. 9), i.e. the ratio of saturation remanence to saturation magnetization (M_{rs}/M_s) against the ratio of remanent coercive force to coercive force (H_{cr}/H_c). For this, we used the parameters from the hysteresis loops of Fig. 8 and the value of H_{cr} from the associated remanence curves. The best fit to a power-law of the Ponón Trehué data defines the relation: $M_{rs}/M_s = 0.41(H_{cr}/H_c)^{-0.70}$ (see Fig. 9). Our data fall in the region between SD + MD and SP + SD mixing curves for magnetite, and follows the trend of PSD + SP mixing curves (Dunlop, 2002b). Despite that a contribution of other magnetic minerals cannot be neglected, the Day plot is probably indicating the presence of ultrafine grains of magnetite for the samples of the Ponón Trehué Formation in consistence with the other magnetic properties already determined. All samples of the Ponón Trehué Formation fall in the field defined by Katz et al. (2000) for remagnetized limestones, and follow a trend parallel to those described by Jackson (1990b), Channell and McCabe (1994) and Trindade et al. (2004) for other remagnetized carbonates. The hysteresis results of the middle Cambrian to early Ordovician carbonates (limestones to dolomites) of the Eastern Precordillera (San Juan province), previously studied by Rapalini et al. (2000), are also shown in the Day-type plot of Fig. 9. Carbonates from La Flecha, La Silla and San Juan Formation are interpreted as remagnetized by the Sanrafaelic overprint, whereas carbonates coming from La Laja and Zonda Formations are unremagnetized. Magnetite has been interpreted as the carrier of the remagnetization at this area, although a detailed rock magnetic study is still lacking. The data from unremagnetized carbonates fall along the SD + MD trend for magnetite-theoretical curves (Dunlop, 2002a), far from the Ponón Trehué values, whereas the remagnetized carbonates are broadly distributed from the SD + MD to PS + SD trends (Rapalini et al., 2000; Font et al., 2012). The samples of the Ponón Trehué Formation have M_{rs}/M_s ratios similar to those of the remagnetized limestones of the San Juan Formation. Other units from the Precordillera seem not to fall in the "remagnetized carbonates" area of the plot. Further rock magnetic studies on these units are needed.

In order to further characterize the carriers of the Sanrafaelic overprint, an IRM was acquired up to 452 mT in one sample per site in order to reach the saturation of the lower coercivity phases (magnetite and pyrrhotite). Though a contribution to the total IRM from higher coercivity phases (haematite and goethite) is probably present, it is expected to be small or negligible. The crossover plots (IRM acquisition and AF demagnetization of IRM as a function of the applied field, Fig. 10) determined the intersection points *R* with abscissas ranging from 62 to 126 mT and ordinates bracketed

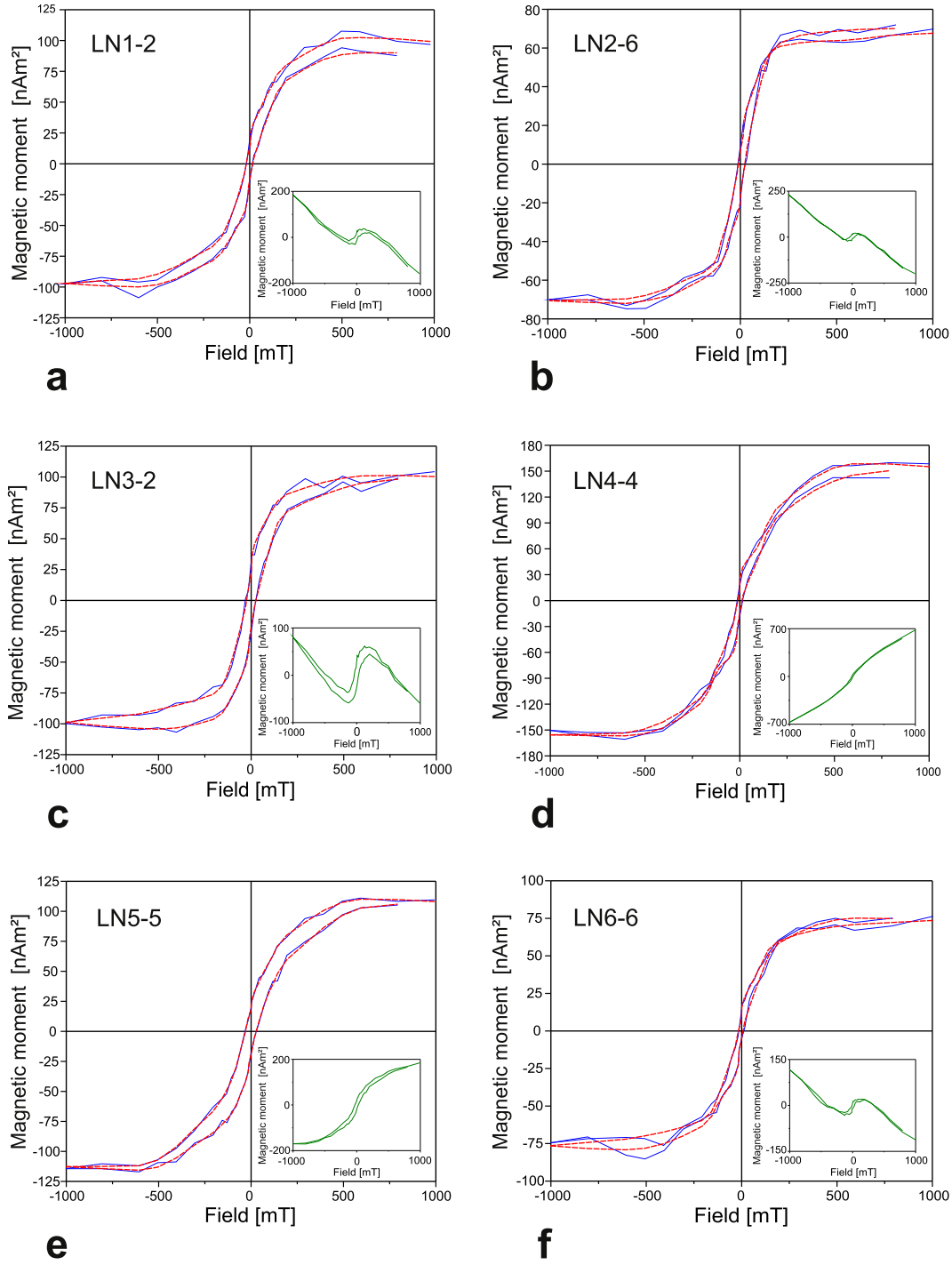

Fig. 8. Hysteresis loops of the Ponón Trehué remagnetized carbonate rocks after subtraction of diamagnetic and paramagnetic contribution (blue). The insets show measured loops before correction (green). Red dashed line: smoothed curve. (For interpretation of the references to colour in this figure legend, the reader is referred to the web version of this article.)

between 0.34 and 0.46. The *R* value is indicative of the effective grain-size of the magnetic minerals and, in the case of the samples from the Ponón Trehué Formation, it is consistent with PSD (LN3-5 and LN6-6m) or SD (LN1-4b, LN2-4, LN4-2m and LN5-6m) pyrrhotite (Symons and Cioppa, 2000). The almost symmetrical shape of the IRM acquisition and IRM demagnetization curves indicates weakly to non-interacting particles (Cisowski, 1981) for all the specimens, except for sample LN6-6A, for which a higher interaction is observed. On the other side, for all samples (Fig. 10), the modified Lowrie-Fuller test (Johnson et al., 1975) shows that the ARM is less stable to demagnetization than the IRM implying the dominance of a coarse-grained fraction. These contrasting results that typify the behaviour of magnetite-bearing remagnetized carbonates (Lowrie and Heller, 1982; Jackson, 1990b) were also observed in remagnetized carbonates containing magnetite plus pyrrhotite and haematite (Trindade et al., 2004; Font et al., 2006), supporting again the combined contribution of these minerals in the Ponón Trehué limestones.

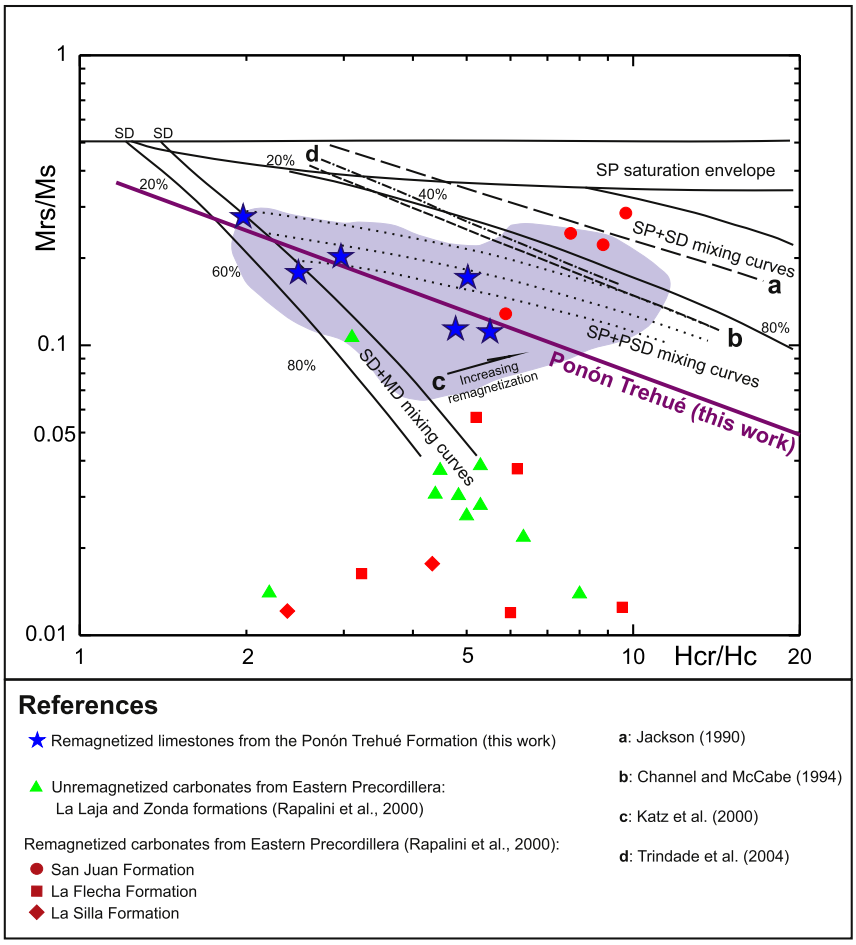

Fig. 9. Hysteresis data from the Ponon Trehue Formation plotted on the theoretical unmixing diagram of Dunlop (2002a, b) with worldwide fitted curves of remagnetized carbonates and the field of remagnetized limestones from Katz et al. (2000) indicated as a shaded area (modified from Font et al., 2012). Data from unremagnetized/remagnetized carbonates from Precordillera are also shown (Rapalini et al., 2000) A fitted power-law for the Ponón-Trehué samples is indicated.

4.3. Magnetic fabrics

The magnetic fabrics of the remagnetized limestones were studied by means of the anisotropy of magnetic susceptibility and the anisotropy of anhysteretic remanent magnetization.

All susceptibility ellipsoids are well-resolved (Fig. 11). The average magnetic susceptibility k_m is very low for all sites ($-4.9 \times 10^{-6} \leq k_m \leq 1.6 \times 10^{-5}$ SI, Table 3). All specimens from sites LN1, LN2 and LN3 are diamagnetic. From the remaining sites only two specimens from site LN6 are also diamagnetic. These are ruled out from the analysis because their susceptibility parameters are clearly discordant with respect to the others from the same site. The anisotropy degree (P) varies between ~1.04 and ~1.14 for the susceptibility ellipsoid and its shape ranges from slightly (site LN6) to strongly prolate (site LN3).

Remanence ellipsoids from sites LN3, LN4, LN5 and LN6 are well-resolved, while principal directions from sites LN1 and LN2 are widely dispersed (Fig. 11). The latest sites are characterized by negative values of average bulk susceptibility (~-4×10^{-6} SI, Table 3) revealing that the content of ferrimagnetic grains is probably too scarce to accurately define the remanence ellipsoid. For most of the following analysis, sites LN1 and LN2 are excluded. The average anhysteretic susceptibility k_a is bracketed between 3.9×10^{-5} and 1.5×10^{-4} SI (Table 3). The anisotropy degree ranges between ~1.08 and ~1.24 for the remanence ellipsoid and it is always higher than the corresponding one for the AMS fabric. The shape parameter is lower than the associated AMS fabric and it varies from slightly (site LN6) to moderately prolate (site LN5).

The AMS ellipsoids are characterized by a normal fabric, i.e. K_3 normal to the bedding plane (Fig. 11) with K_1 ranging from subhorizontal to high inclinations. Clustering of K_1 axis and elongation of K_3 axes distributions (i.e. LN4, LN5) strongly suggest some tectonic overprint of the AMS fabric. The tectonic origin of the ferromagnetic fabric is more evident in the AARM ellipsoids. Although samples LN1 and LN2 do not show a coherent fabric, the others present a magnetic lineation parallel to the fold axis (star in Fig. 11), which confirms an association of the remanence carriers fabric with fold development. This is further confirmed by maximum ARM axes oblique to the bedding plane in samples LN3 and LN4, strongly suggesting ferromagnetic mineral formation under local stress regime associated to folding.

Statistical analyses (Jelínek, 1978) of AMS and AARM fabrics were applied to the entire collection of specimens in *in situ* coordinates (Fig. 12a, d and g), after 21% untilting, which is the percentage of the highest improving of clustering of palaeomagnetic directions according to the fold test (Fig. 12b, e and f), and after full bedding correction (Fig. 12c, f and i). Statistical analysis without diamagnetic samples (Fig. 12d, e and f) was also considered. It is observed that directions of the AMS ellipsoid that contain the diamagnetic samples are more dispersed.

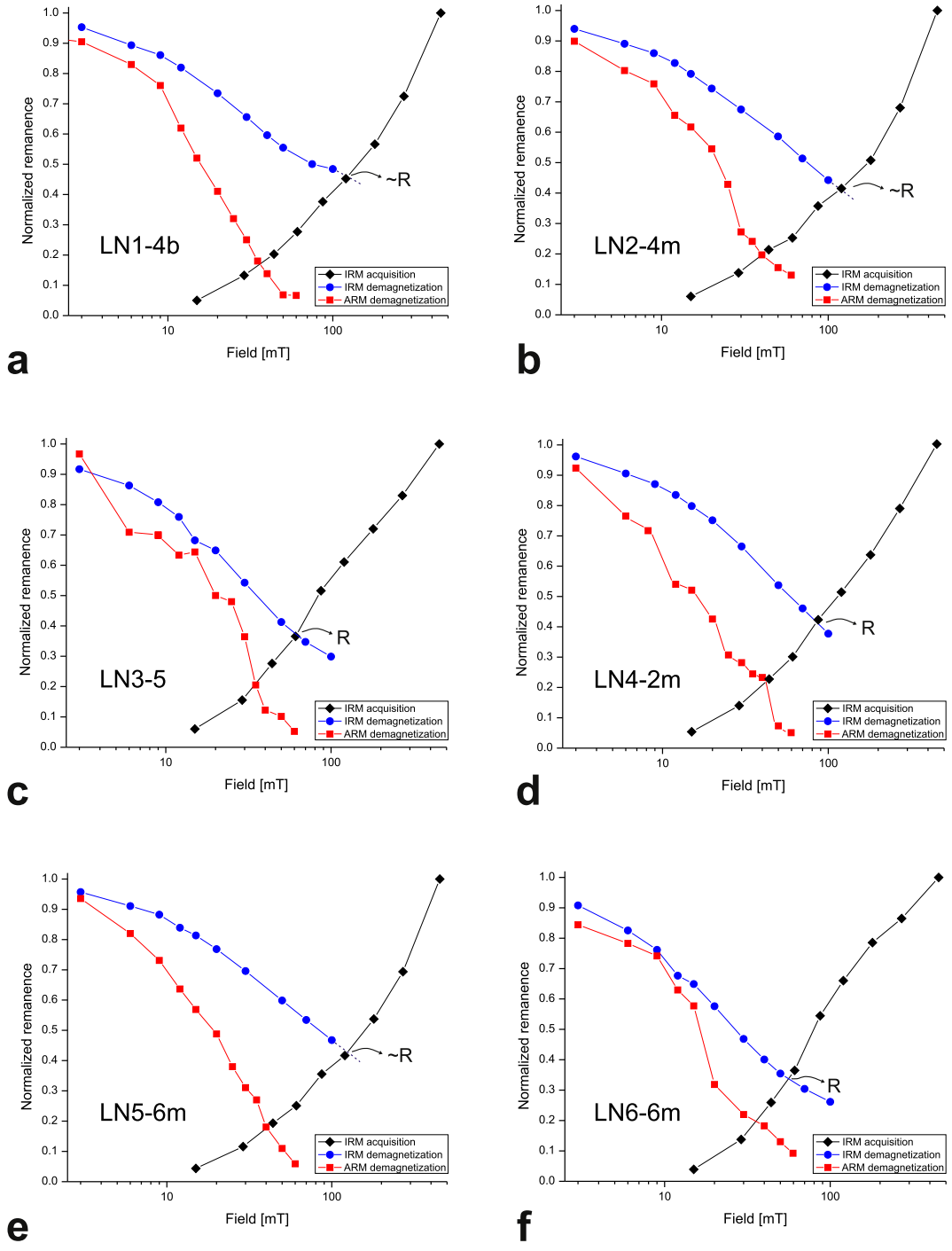

Fig. 10. Curves of the modified Lowrie-Fuller (Johnson et al., 1975) and Cisowski (1981) tests for the limestones of the Ponón Trehué Formation.

From Fig. 12 (Table 4), it is observed that the hinge line of the fold (plunge 15°; Az. 150°) is coincident with the mean K_1 direction of the AARM ellipsoid in geographic coordinates and at 21% tectonic correction (declination 144.1°, inclination 25.4° and declination 144.1°, inclination 24.6°, respectively). As already mentioned, the magnetic lineation subparallel to the fold axis suggests that the origin of the fabric, and likely the magnetic carriers (magnetite plus pyrrhotite), is not primary, but associated with the folding process. This is more easily explained if new magnetic minerals were chemically precipitated during the deformational (Sanrafaelic) event that affected the region.

5. Discussion

The position of the PT pole (Truco and Rapalini, 1996) is indicated in Fig. 13, where poles of the late Palaeozoic-early Mesozoic for South America together with the remagnetized Sanrafaelic poles from Precordillera are also indicated. The PT palaeopole position is close to the late Carboniferous-early Permian poles which is consistent with the early Permian age of deformation of Ponón Trehué Formation due to the Sanrafaelic orogenic phase. This tectonic phase resulted in the inversion and folding of the Carboniferous-early Permian deposits of the back-arc basins of

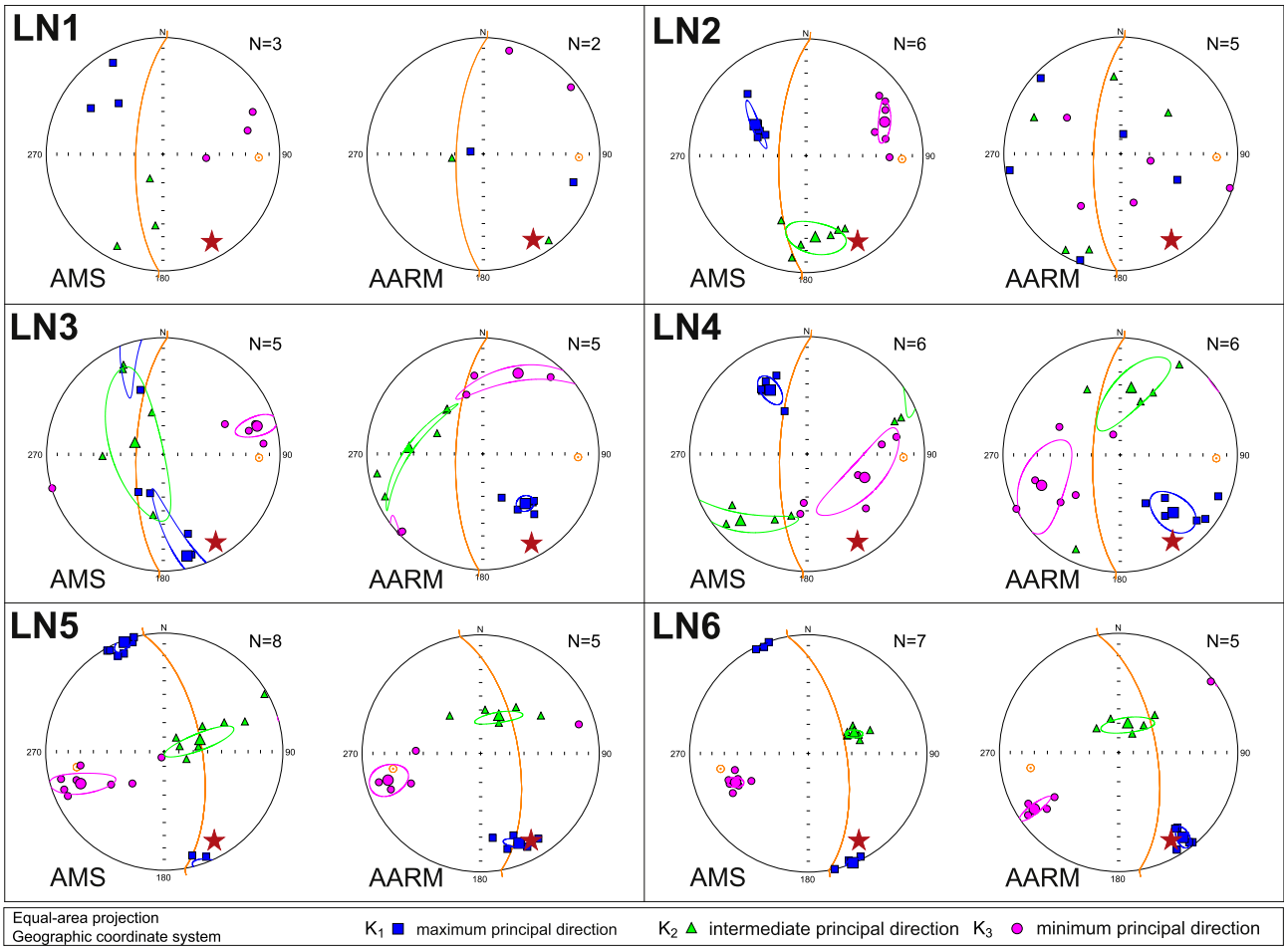

Fig. 11. Anisotropy of low-field AC magnetic susceptibility (AMS) and anisotropy of anhysteretic remanent magnetization (AARM) plots in equal-area projections (lower hemisphere) in the geographic coordinate system for each sampling site. The ellipses correspond to 95% confidence regions of the mean axes (Jelínek, 1978). Projections of the bedding plane and pole to the bedding are indicated (orange). The red star points out the orientation of the hinge line. (For interpretation of the references to colour in this figure legend, the reader is referred to the web version of this article.)

Table 3
Site-mean AMS and AARM parameters. n: number of measured specimens; k_m: magnetic susceptibility (in 10^{-6} SI); k_a: anhysteretic susceptibility (in 10^{-5} SI); P: anisotropy parameter; L: magnetic lineation; F: magnetic foliation; T: shape of anisotropy ellipsoid.

Site	AMS fabric						AARM fabric					
	n	k_m [10^{-6}(SI)]	P	L	F	T	n	k_a [10^{-5}(SI)]	P	L	F	T
LN1	3	−3.8	–	–	–	–	2	6.3	–	–	–	–
LN2	6	−4.0	1.036	1.020	1.016	−0.112	5	4.1	–	–	–	–
LN3	5	−4.9	1.037	1.030	1.004	−0.754	5	3.9	1.143	1.088	1.050	−0.268
LN4	6	12.9	1.048	1.036	1.012	−0.493	6	7.6	1.077	1.043	1.033	−0.136
LN5	8	16.1	1.103	1.078	1.023	−0.533	5	14.5	1.172	1.116	1.050	−0.388
LN6	7	8.6	1.136	1.071	1.061	−0.076	5	4.5	1.238	1.121	1.105	−0.066

Río Blanco, Calingasta-Uspallata and San Rafael (see López Gamundí et al., 1994 and references therein). Tectonic shortening of 60–70% were reported in areas of the Frontal Cordillera (Heredia et al., 1996). It was followed by an extensive, mainly rhyolitic volcanism of the Choiyoi Group (see Mpodozis and Kay, 1992). A mean age of 280 Ma is accepted for this important tectonic phase (Azcuy and Caminos, 1987; López Gamundí et al., 1994; Llambías and Sato, 1995; Kleiman and Japas, 2009; Domeier et al., 2011; Rocha-Campos et al., 2011). This is supported by field evidence at the Ponón Trehué area, where the late Permian volcanic and pyroclastic rocks of the Cerro Carrizalito Group show an important angular unconformity and are not affected by late Palaeozoic folding. Therefore, a ca. 280 Ma age was assumed for PT (Truco, 1996; Truco and Rapalini, 1996). Fig. 13 also shows the palaeomagnetic poles from the Alcaparrosa Formation (AL; Vilas and Valencio, 1978; reinterpreted by Rapalini and Tarling, 1993), the Hoyada Verde Formation (HV, Rapalini and Vilas, 1991), the San Juan Limestones (SJ, Rapalini and Tarling, 1993) and the La Flecha Formation (Rapalini and Astini, 2005). All these poles, with the possible exception of the Alcaparrosa Formation (see Geuna and Escosteguy, 2006), have been calculated from remagnetized rocks during the San Rafaelic

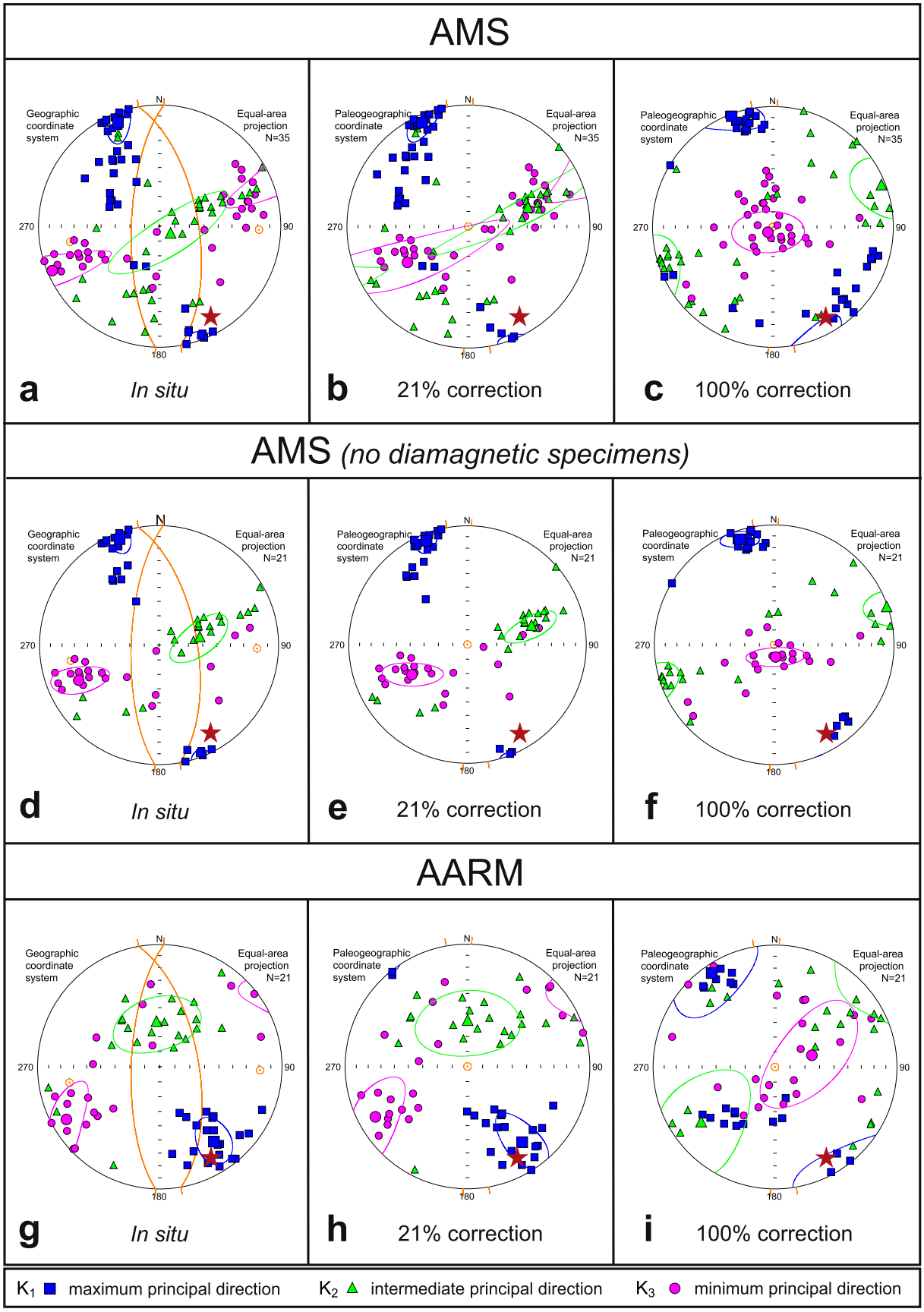

Fig. 12. AMS plots in equal-area projections (lower hemisphere) for the entire collection of specimens of the Ponón Trehué Formation. AARM plots in equal-area projections (lower hemisphere) comprise specimens from sites LN3, LN5 and LN6. Results of AMS data excluding specimens with diamagnetic bulk susceptibility are presented separately in d), e) and f). The ellipses correspond to 95% confidence regions of the mean axes (Jelínek, 1978). a), d) and g) In geographic coordinate system. b), e) and h) Idem, after partial (21%) tilt correction. c), f) and i) Idem, after 100% tectonic correction. Projections of the bedding plane and pole to the bedding are indicated (orange). The red star points out the orientation of the hinge line. (For interpretation of the references to colour in this figure legend, the reader is referred to the web version of this article.)

Table 4
Principal axes directions of mean AMS and AARM ellipsoids for the complete set of specimens (Fig. 12). Confidence angles are indicated between brackets. AMS data are shown with and without diamagnetic specimens. Directions are shown in the geographic coordinate system, at 21% tilt corrected and 100% tilt corrected.

Fabric	Coordinate system	n	K_1		K_2		K_3	
			Dec [°]	Inc [°]	Dec [°]	Inc [°]	Dec [°]	Inc [°]
AMS (all specimens)	Geographic	35	339.6 (13.0)	6.1 (5.6)	81.1 (23.9)	61.7 (0.6)	246.4 (23.4)	27.5 (7.7)
	Palaeogeographic (21% corrected)	35	335.9 (14.2)	7.2 (7.2)	73.8 (74.8)	47.7 (7.7)	239.5 (74.8)	41.4 (13.3)
	Palaeogeographic (full corrected)	35	339.6 (20.0)	2.1 (10.5)	69.7 (24.7)	4.4 (15.4)	223.8 (24.7)	85.1 (14.0)
AMS (non-diamagnetic specimens)	Geographic	21	339.6 (13.0)	6.1 (5.6)	81.1 (23.9)	61.7 (10.6)	246.4 (23.4)	27.5 (7.7)
	Palaeogeographic (21% corrected)	21	338.6 (10.3)	6.8 (5.5)	75.0 (21.4)	43.5 (6.8)	241.6 (22.0)	45.7 (7.6)
	Palaeogeographic (full corrected)	21	342.0 (11.1)	8.2 (6.5)	72.2 (20.1)	1.6 (8.6)	173.0 (20.1)	81.6 (6.4)
AARM	Geographic	21	144.1 (19.3)	25.4 (9.8)	355.7 (29.5)	60.9 (18.2)	240.6 (29.0)	13.3 (10.1)
	Palaeogeographic (21% corrected)	21	144.1 (27.0)	24.6 (9.7)	0.1 (34.4)	60.4 (22.5)	241.3 (32.7)	15.3 (13.4)
	Palaeogeographic (full corrected)	21	326.0 (28.7)	7.8 (22.5)	232.4 (45.7)	24.5 (23.8)	72.4 (45.0)	64.1 (21.2)

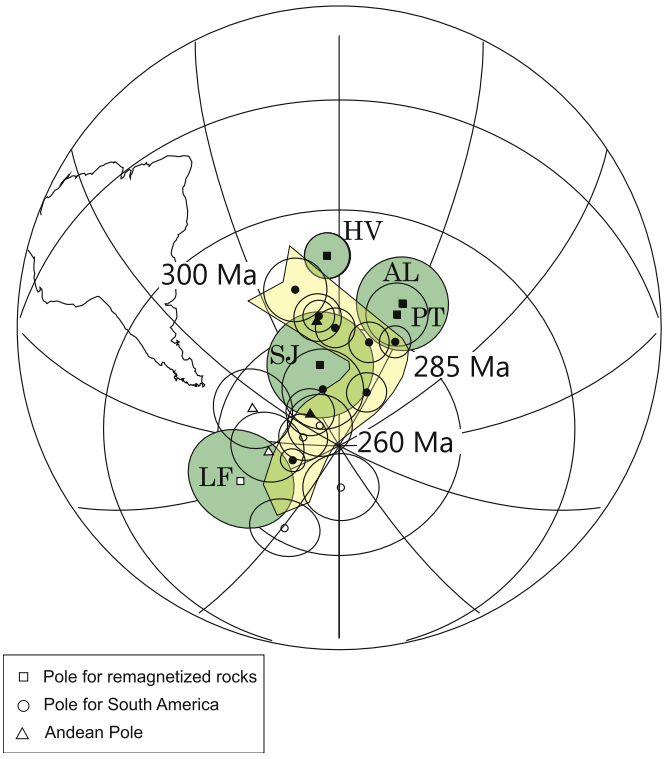

Fig. 13. Apparent polar wander path (APWP) of the late Carboniferous-early Triassic for South America and palaeomagnetic poles from remagnetized units during the Sanrafaelic tectonic phase (squares) from Precordillera (SJ, LF, AL and HV) and the San Rafael Block (PT). The palaeomagnetic poles that define the APWP are indicated by triangles and circles. Full (open) symbols point out reverse (mixed) polarities. Ovals of 95% confidence are shown. Poles: SJ, San Juan (Rapalini and Tarling, 1993); LF, La Flecha (Rapalini and Astini, 2005); PT, Ponón Trehué (Truco and Rapalini, 1996); AL, Alcaparrosa (Rapalini and Tarling, 1993); HV, Hoyada Verde (Rapalini and Vilas., 1991). Taken from Rapalini and Astini (2005).

tectonic phase, and all them lie close to the late Carboniferous–early Permian South American poles.

Origin of regional remagnetizations have been widely debated for several decades (see Van der Voo and Torsvik, 2012 and references therein). In general, three main mechanisms have been proposed for remagnetizations, i) thermoviscous remanence (Kent, 1985), ii) chemical remagnetization due to burial diagenesis and "*in situ*" clay alteration (e.g. Katz et al., 1998; Gill et al., 2002; Trindade et al., 2004; Kodama, 2012) and iii) chemical remagnetization associated to fluid migrations, like chemically active brines expelled from orogenic areas (Oliver, 1986; Bethke and Marshak, 1990) or hydrothermal environments (e.g. Nelson et al., 2002). The Sanrafelic remagnetization was firstly proposed by Rapalini and Tarling (1993) who presented evidence of a chemical remagnetization that was linked to hypothetical fluid migration expelled towards the East from the late Palaeozoic marine basins of Western Argentina when inverted and deformed in the late early Permian by the San Rafael Orogeny. Rapalini and Astini (2005) further insisted in such model considering that a pattern of progressive age of remagnetization can be identified in the Precordillera of Western Argentina. They assessed polar positions, age of magnetization with respect to folding, polarities and geographical distribution of the remagnetized units and suggested a temporal-spatial migration pattern in which the geologic units in the Western Precordillera were remagnetized during early Permian while the Eastern Precordillera units were remagnetized during late Permian, hypothetically as a consequence of fluids expelled from the orogenic area. However, these ideas have yet to be supported on detailed mineralogical and rock magnetic studies.

We found that the Sanrafaelic remagnetization at the Ponón Trehué area is carried by magnetite and pyrrhotite, though recent formation of high coercivity minerals (goethite and subordinately haematite) also was detected. The precise origin of the latest minerals is not certain, but it is likely related to weathering, as suggested by the remanence direction associated to them coincident with the Earth Magnetic Field Dipole at the study locality, and which are therefore devoid of any relation with the Sanrafaelic remagnetization. Goethite in carbonate rocks has been related to the oxidation of sulphides (pyrrhotite, in this study) during weathering (Zwing et al., 2005). Diverse magnetic studies in the Ponón Trehué rocks (hysteresis parameters, frequency dependence of susceptibility, Cisowski and modified Lowrie-Fuller tests) support the presence of ultrafine grains (SP magnetite) formed during chemical processes. NRM and three-axis IRM demagnetization indicate that pyrrhotite is another important contributor to the remanence. This and the results of the magnetic fabric analyses indicate an authigenic origin of the magnetic minerals during folding associated with the Sanrafaelic tectonic phase. The evaluated magnetic properties are compatible with the proxies of remagnetization in magnetite-bearing carbonate rocks. In fact, the diagnostic properties of remagnetized carbonates were also observed in many multi-mineralic rocks (Weil and Van der Voo, 2002; Zegers et al., 2003; Trindade et al., 2004; Zwing et al., 2005; Font et al., 2006; Oliva-Urcia and Pueyo, 2007), though with some limitations (Jackson and Swanson-Hysell, 2012). These considerations rule out a thermoviscous origin for the remagnetization. Whether the remanence-carrying minerals in the Ponón Trehué Formation are the product of *in situ* clay transformations or of precipitation associated to "orogenic" or "hydrothermal" fluids is more difficult to assess, in part due to the small-scale nature of our study. Despite this, some further considerations can be made. One significant fact is that both magnetite and pyrrhotite carry the same magnetic syntectonic

component suggesting a coeval or nearly coeval remanence acquisition and therefore mineral formation. Secondary origin of pyrrhotite in limestone has been ascribed to pyrite oxidation (e.g. Salmon et al., 1988). Oxidizing brines can in that way be responsible for the origin of both pyrrhotite and magnetite. Katz et al. (1998) demonstrated that in many remagnetized limestones, secondary magnetite was created in the alteration process of smectite into illite due to burial diagenesis. However, such mechanism has not been proposed for pyrrhotite formation. This suggests that the origin of remanence from chemically active circulating fluids during tectonic deformation is the first candidate for the Ponón Trehué remagnetization.

The ca. 280 Ma of the San Rafael tectonic phase suggests a similar age for final stages of folding at the Ponón Trehué area, as already mentioned, and for pyrrhotite and magnetite generation. Rubinstein et al. (2004) dated in 279 Ma an event of ore vein mineralization that included significant lead mobilization with associated hydrothermal systems in the San Rafael block few tens of km away from our study area. This appears just as one example of a significant number of ore deposits in the San Rafael Block of similar age and related to arc-magmatism approximately coetaneous with the San Rafael Orogeny. Although the largest outcrops of the Choiyoi rhyolitic magmatic province ("Upper Choiyoi") developed after the San Rafael phase, magmatism coetaneous with final stages of tectonic deformation likely occurred in the region ("Lower Choiyoi" units, Kleiman and Japas, 2009), and should be investigated whether it may be related to remagnetization of limestones.

Progression of remagnetization towards the East, as proposed by Rapalini and Astini (2005), would support the presence of migrating "orogenic fluids" as causing the remagnetization, however Geuna and Escosteguy (2006) showed that the Permian remagnetization of the volcano-sedimentary Ordovician Alcaparrosa Formation, exposed in Western Precordillera, is likely related to a local alteration halo around a Permian intrusion. Furthermore, Rapalini and Tarling (1993) showed a "syntectonic" nature for the remagnetization of these rocks. This suggests that while the migrating "orogenic" fluids can explain most regional aspects of the Sanrafaelic magnetization, the role of coetaneous magmatism should be investigated deeply.

6. Conclusions

Palaeomagnetic, magnetic fabric and rock-magnetic studies were carried out on remagnetized Middle-Ordovician limestones from the Ponón Trehué Formation (San Rafael Block, central-western Argentina). This magnetization, which was acquired during folding of the rocks in the early Permian due to the San Rafael orogeny, constitutes new evidence on the broad character of the Sanrafaelic overprint. Though this late Palaeozoic widespread remagnetization event has been known for many years, experiments on magnetic properties of sedimentary rocks affected by this process were very restricted. Our studies revealed that the limestones from the Ponón Trehué Formation carry a secondary characteristic magnetization residing in pyrrhotite and magnetite. Evidence of other magnetic minerals (goethite, haematite), of recent formation, was found too. The standard worldwide magnetic properties used as signature of remagnetization in carbonate rocks were also recognized in these multimineralic limestones: high frequency-dependent magnetic susceptibility, wasp-waisted shape of hysteresis loops, abnormally high hysteresis ratios and contradictory Lowrie-Fuller and Cisowski tests. These characteristics are indicative of the presence of ultrafine ferromagnetic grains suggesting that the Sanrafaelic orogeny triggered a chemical remagnetization process synchronous with folding that originated the formation of authigenic magnetic material. This origin for the remagnetization is confirmed by the magnetic fabric analyses which shows evidence of magnetic grains developed under the local stress regime responsible for folding. Although the previously proposed model of a remagnetization triggered by chemically active (oxidizing?) fluids expelled from the orogen as it developed in the early Permian is a viable explanation for the Sanrafaelic remagnetization, the role of the nearly coeval extended magmatism in Precordillera and the San Rafael Block remains to be properly evaluated.

Further rock-magnetic studies on samples from the early Cambrian to mid-Ordovician carbonate platform of the Argentine Precordillera affected by the pervasive Sanrafaelic remagnetization event are under way in order to better characterize the nature of this widespread process.

Acknowledgements

We would like to thank Telma S. Berquo for measurements of hysteresis loops and remanence curves at the Instituto de Astronomia, Geofísica e Ciências Atmosféricas (Universidade de São Paulo, Brazil) by using a Molspin vibrating sample magnetometer. We greatly appreciate technical support by Carlos Vasquez and Matías Naselli. This work was financially supported by Agencia Nacional de Promoción Científica y Tecnológica (PICT-2011-0956 grant). We gratefully acknowledge two anonymous reviewers for their constructive comments which significantly improved the manuscript as well as Associate Editor Camilo Montes.

Appendix 1

Acquisition of ARM (anhysteretic remanent magnetization) in selected samples from the Ponón Trehué Formation up to 500 μT of H_{dc} field (H_{ac} = 100 mT). Inset: normalized curves. An almost linear dependence is expected for fields (H_{dc}) lower than 50 μT.

The study of ARM indicated that the linear dependence of the anhysteretic magnetization with H_{dc} field is valid up to ~50 μT. Below this limit, the available H_{dc} field that produces our magnetizer ($\leq$ 30 μT) imparts low values of anhysteretic magnetization to the samples. For this reason, we selected H_{dc} = 50 μT considering that a departure from the linear dependence would probably be small enough to be neglected.

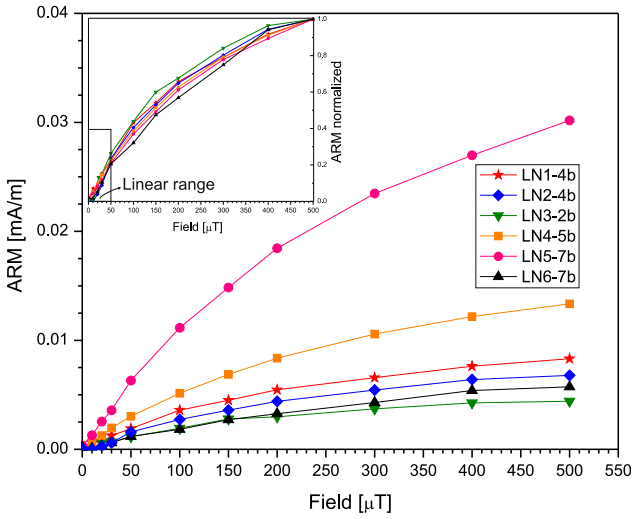

Appendix 2

Variation of bulk magnetic susceptibility with an external magnetic AC field with H_{peak} from 2 to 700 Am^{-1} at a fixed frequency of 976 Hz for twelve remagnetized samples from the Ponón Trehué Formation.

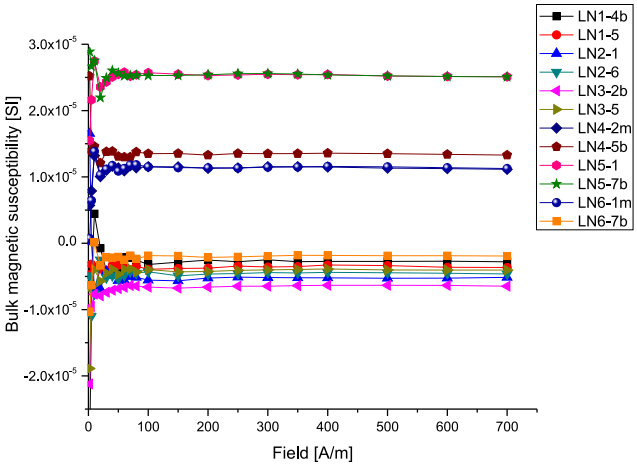

References

Abre, P., Cingolani, C., Zimmermann, U., Cairncross, B., Chemale, F., 2011. Provenance of Ordovician clastic sequences of the San Rafael Block (Central Argentina), with emphasis on the Ponón Trehué Formation. Gondwana Res. 19, 275–290.

Astini, R.A., Ramos, V.A., Benedetto, J.L., Vaccari, N.E., Cañas, F.L., 1996. La Precordillera: un terreno exótico a Gondwana. In: XIII Congreso Geológico Argentino y III Congreso de Exploración de Hidrocarburos, Buenos Aires. Actas 5, pp. 293–324.

Astini, R.A., Benedetto, J.L., Vaccari, N.E., 1995. The early Paleozoic evolution of the Argentine Precordillera as a Laurentian rifted, drifted and collided terrane: a geodynamic model. Geol. Soc. Am. Bull. Geol. Soc. Am. Bull. 107 (3), 253–273.

Astini, R.A., 2002. Los conglomerados basales del Ordovícico de Ponón Trehué (Mendoza) y su significado en la historia sedimentaria del terreno exótico de Precordillera. Rev. Asoc. Geol. Argent. 57 (1), 19–34.

Azcuy, C.L., Caminos, R., 1987. Diastrofismo. In: Archangelsky, S. (Ed.), El Sistema Carbonífero en la República Argentina. Academia Nacional de Ciencias Córdoba, Córdoba, pp. 239–252.

Baldis, B., Blasco, G., 1973. Trilobites ordovícicos de Ponón Trehué, Sierra Pintada de San Rafael, provincia de Mendoza. Ameghiniana 10 (1), 72–88.

Beresi, M.S., Heredia, S., 2003. First occurrence of Epiphyton, cyanobacteria from the Middle Ordovician of the Ponón Trehué, Mendoza province, Argentina. In: Albanesi, G.L., Beres,i, M.S., Peralta, S.H. (Eds.), Ordovician from the Andes, Serie Correlación Geológica 17. INSUGEO, San Miguel de Tucumán, pp. 257–261.

Bethke, C.M., Marshak, S., 1990. Brine migrations across North America-The plate tectonics of groundwater. Annu. Rev. Earth Planet. Sci. 18, 287–315.

Bina, M., Daly, L., 1994. Mineralogical change and self-reversed magnetizations in pyrrhotite resulting from partial oxidation; geophysical implications. Phys. Earth Planet. Inter 85 (1–2), 83–99.

Bobbio, M.L., Rapalini, A.E., Vilas, J.F., 1990. Estudio paleomagnético preliminar de la Formación Hoyada Verde, Precordillera de San Juan: un ejemplo de remagnetización sintectónica. Rev. Geol. Chile 17 (2), 191–200.

Bordonaro, O., Keller, M., Lehnert, O., 1996. El Ordovícico de Ponón Trehué en la Provincia de Mendoza (Argentina): redefiniciones estratigráficas. In: XIII Congreso Geológico Argentino y III Congreso de Exploración de Hidrocarburos, Buenos Aires. Actas 1, pp. 541–550.

Cingolani, C., Varela, R., 1999. The San Rafael Block, Mendoza (Argentina). Rb–Sr isotopic age of basement rocks. In: II South American Symposium on Isotope Geology, Anales, pp. 23–26.

Cingolani, C.A., Llambías, E.J., Basei, M.A.S., Varela, R., Chemale Jr., F., Abre, P., 2005. Grenvillian and Famatinian-age igneous events in the San Rafael Block, Mendoza province, Argentina: geochemical and isotopic constraints. In: Gondwana 12 Conference, Geological and Biological Heritage of Gondwana, Mendoza, Abstracts, p. 102.

Cisowski, S., 1981. Interacting vs. non-interacting single domain behavior in natural and synthetic samples. Phys. Earth Planet. Inter 26 (1–2), 56–62.

Channell, J.E.T., McCabe, C., 1994. Comparison of magnetic hysteresis parameters of unremagnetized and remagnetized limestones. J. Geophys. Res. 99 (B3), 4613–4623.

Criado Roque, P., Ibañez, G., 1979. Provincia geológica Sanrafaelino-pampeana. In: Segundo Simposio de Geología Regional Argentina. Actas 1. Academia Nacional de Ciencias, Córdoba, pp. 837–869.

Cuerda, A., Cingolani, C., 1998. El Ordovícico de la región del cerro Bola en el Bloque San Rafael, Mendoza: sus faunas graptolíticas. Ameghiniana 35 (4), 427–448.

Day, R., Fuller, M., Schmidt, V.A., 1977. Hysteresis properties of titanomagnetites: grain size and composition dependence. Phys. Earth Planet. Inter 13 (4), 260–267.

Dearing, J.A., Dann, R.J.L., Hay, K., Lees, J.A., Loveland, P.J., Maher, B.A., O'Grady, K., 1996. Frequency-dependent susceptibility measurements of environmental materials. Geophys. J. Int. 124 (1), 228–240.

Domeier, M., Van der Voo, R., Tohver, E., Tomezzoli, R.N., Vizan, H., Torsvik, T.H., Kirshner, J., 2011. New Late Permian paleomagnetic data from Argentina: refinement of the apparent polar wander path of Gondwana. Geochem. Geophys. Geosyst. 12 (7), Q07002.

Dunlop, D.J., 2002a. Theory and application of the Day plot (Mrs/M s versus Hcr/Hc) 1. Theoretical curves and tests using titanomagnetite data. J. Geophys. Res. 107 (B3), 2056.

Dunlop, D.J., 2002b. Theory and application of the Day plot (Mrs/Ms versus Hcr/Hc) 2. Application to data for rocks, sediments, and soils. J. Geophys. Res. 107 (B3), 2057.

Dunlop, D.J., Özdemir, Ö., 2000. Effect of grain size and domain state on thermal demagnetization tails. Geophys. Res. Lett. 27 (9), 1311–1314.

Fisher, R., 1953. Dispersion on a sphere. Proc. R. Soc. Lond. A217 (1139), 295–305.

Font, E., Trindade, R.I.F., Nédélec, A., 2006. Remagnetization in bituminous limestones of the Neoproterozoic Araras Group (Amazon craton): hydrocarbon maturation, burial diagenesis, or both? J. Geophys. Res. 111 (B06204).

Font, E., Neto, C.F.P., Ernesto, M., 2011a. Paleomagnetism and rock magnetism of the Neoproterozoic Itajaí Basin of the Rio de la Plata craton (Brazil): Cambrian to Cretaceous widespread remagnetizations of South America. Gondwana Res. 20 (4), 782–797.

Font, E., Youbi, N., Fernandes, S., El Hachimi, H., Kratinová, Z., Hamim, Y., 2011b. Revisiting the magnetostratigraphy of the Central Atlantic Magmatic province (CAMP) in Morocco. Earth Planet. Sci. Lett. 309 (3–4), 302–317.

Font, E., Rapalini, A.E., Tomezzoli, R.N., Trindade, R.I.F., Tohver, E., 2012. Episodic remagnetizations related to tectonic events and their consequences for the South America polar wander path. In: Elmore, R.D., Muxworthy, A.R., Aldana, M.M., Mena, M. (Eds.), Remagnetization and Chemical Alteration of Sedimentary Rocks, Geol. Soc. London, Spec. Publ. 371, pp. 55–87.

Geuna, S.E., Escosteguy, L.D., 2006. Mineralogía magnética de la Formación Alcaparrosa (Ordovícico) y del pórfiro pérmico que la intruye, Calingasta, provincia de San Juan. In: VIII Congreso de Mineralogía y Metalogenia (MINMET 2006), Facultad de Ciencias Exactas y Naturales, Buenos Aires, Actas, pp. 99–106.

Gialanella, P.R., Heller, F., Incoronato, A., 1994. Rock magnetism of deformed Upper triassic limestones from the Lagonegro Basin (Southern Apennines, Italy). Geophys. Res. Lett. 21 (24), 2665–2668.

Gill, J.D., Elmore, R.D., Engel, M.H., 2002. Chemical remagnetization and clay diagenesis: testing the hypothesis in the Cretaceous sedimentary rocks of northwestern Montana. Phys. Chem. Earth 27 (25–31), 1131–1139.

Heredia, S., 1982. Pygodus anserinus Lamont et Lindström (Conodonto) en el Llandeillano de la Formación PonónTrehué. Ameghiniana 19 (3–4), 101–104 (Buenos Aires).

Heredia, S., 1996. El Ordovícico del Arroyo Ponón Trehué, sur de la provincia de Mendoza. In: XIII Congreso Geológico Argentino y III Congreso de Exploración de Hidrocarburos, Buenos Aires. Actas 1, pp. 601–605.

Heredia, S., Rosales, C., 2006. Biofacies de Conodontes de la Formación Ponón Trehué y la importancia bioestratigráfica como sección tipo para el límite del Ordovícico Medio-Ordovícico Superior de Cuyania (Argentina). In: Temas de la Geología Argentina I. Serie Correlación Geológica 21. INSUGEO, San Miguel de Tucumán, pp. 7–16.

Heredia, S., 2006. Revisión estratigráfica de la Formación Ponón Trehué (Ordovícico), Bloque de San Rafael, Mendoza. In: Temas de la Geología Argentina I. Serie Correlación Geológica 21. INSUGEO, San Miguel de Tucumán, pp. 59–74.

Heredia, N., Rodriguez Fernández, L.R., Ragona, D., 1996. Structure of the Argentine Andean Cordillera between 30°30′ and 31°00′S. In: Third International Symposium on Andean Geodynamics, St. Malo, Extended Abstracts, pp. 379–382.

Hrouda, F., 2004. Problems in Interpreting AMS Parameters in Diamagnetic Rocks. In: Geol. Soc. London, Spec. Publ. 238, pp. 49–59.

Hrouda, F., Chlupáčová, M., Pokorný, J., 2006a. Low-field variation of magnetic susceptibility measured by the KLY-4S Kappabridge and KLF-4A magnetic susceptibility meter: accuracy and interpretational programme. Stud. Geophys. Geod. 50 (2), 283–299.

Hrouda, F., Chlupáčová, M., Mrázová Š, 2006b. Low-field variation of magnetic susceptibility as a tool for magnetic mineralogy of rocks. Phys. Earth Planet. Inter 154 (3–4), 323–336.

Ihmlé, P.F., Hirt, A.M., Lowrie, W., Dietrich, D., 1989. Inverse magnetic fabric in deformed limestones of the Morcles Nappe, Switzerland. Geophys. Res. Lett. 16 (12), 1383–1386.

Jackson, M., 1990a. Magnetic anisotropy of the Trenton limestone revisited. Geophys. Res. Lett. 17 (8), 1121–1124.

Jackson, M., 1990b. Diagenetic sources of stable remanence in remagnetized paleozoic cratonic carbonates: a rock magnetic study. J. Geophys. Res. 95 (B3), 2753–2761.

Jackson, M., Swanson-Hysell, N.L., 2012. Rock magnetism of remagnetized carbonate rocks: another look. In: Elmore, R.D., Muxworthy, A.R., Aldana, M.M., Mena, M. (Eds.), Remagnetization and Chemical Alteration of Sedimentary

Rocks, Geol. Soc. London, Spec. Publ. 371, pp. 228–251.
Jelínek, V., 1978. Statistical processing of anisotropy of magnetic susceptibility measured on groups of specimens. Stud. Geoph. Geod. 22 (1), 50–62.
Jackson, M., Rochette, P., Fillion, G., Banerjee, S., Marvin, J., 1993. Rock magnetism of remagnetized Paleozoic carbonates: low-temperature behavior and susceptibility characteristics. J. Geophys. Res 98, 6217–6225.
Johnson, H.P., Lowrie, W., Kent, D.V., 1975. Stability of anhysteretic remanent magnetization in Fine and coarse magnetite and Maghemite particles. Geophys. J. Int. 41 (1), 1–10.
Katz, B., Elmore, R.D., Cogoini, M., Ferry, S., 1998. Widespread chemical remagnetization: orogenic fluids or burial diagenesis of clays? Geology 26 (7), 603–606.
Katz, B., Elmore, R.D., Cogoini, M., Engel, M.H., Ferry, S., 2000. Associations between burial diagenesis of smectite, chemical remagnetization, and magnetite authigenesis in the Vocontian trough, SE France. J. Geophys. Res. 105, 851–868.
Kirschvink, J.L., 1980. The least-squares line and plane and the analysis of paleomagnetic data. Geophys. J. R. Astron. Soc. 62 (3), 699–718.
Kent, D.V., 1985. Thermoviscous remagnetization in some Appalachian limestones. Geophys. Res. Lett. 12, 805–808.
Kleiman, L.E., Japas, M.S., 2009. The Choiyoi volcanic province at 34°S-36°S (San Rafael, Mendoza, Argentina): implications for the Late Palaeozoic evolution of the southwestern margin of Gondwana. Tectonophysics 473, 283–299.
Kodama, K., 2012. Paleomagnetism of Sedimentary Rocks: Process and Interpretation, first ed. Blackwell Publishing Ltd., pp. 66–80
Llambías, E.J., Sato, A.M., 1995. El batolito de Colangüil: transición entre orogénesis y anorogénesis. Rev. Asoc. Geol. Argent. 50 (1–4), 111–131.
López Gamundí, O.R., Espejo, I.S., Conaghan, P.J., Powell, C.McA., Veevers, J.J., 1994. Southern South America. In: Veevers, J.J., Powell, C.McA. (Eds.), Permian-triassic Pangean Basins and Foldbelts along the Panthalassan Margin of Gondwanaland, Geological Society of America, Memoirs 184, pp. 281–330.
Lowrie, W., 1990. Identification of ferromagnetic minerals in a rock by coercivity and unblocking temperature properties. Geophys. Res. Lett. 17 (2), 159–162.
Lowrie, W., Heller, F., 1982. Magnetic properties of marine limestones. Rev. Geophys. Space Phys. 20 (2), 171–192.
McCabe, C., Jackson, M., Ellwood, B.B., 1985. Magnetic anisotropy in the Trenton limestone: results of a new technique, anisotropy of anhysteretic susceptibility. Geophys. Res. Lett. 12 (6), 333–336.
McDonough, M.R., Ramos, V.A., Isachsen, C.E., Bowring, S.A., Vujovich, G.I., 1993. Edades preliminares de circones del basamento de la Sierra de Pie de Palo, Sierras Pampeanas Occidentales de San Juan: sus implicancias para el supercontinente Proterozoico de Rodinia. In: 12° Congreso Geológico Argentino y 2° Congreso de Exploración de Hidrocarburos, Mendoza. Actas 3, pp. 340–342.
McFadden, P.L., 1990. A new fold test for palaeomagnetic studies. Geophys. J. Int. 103 (1), 163–169.
Mpodozis, C., Kay, S.M., 1992. Late paleozoic to triassic evolution of the Gondwana margin: evidence from Chilean Frontal Cordilleran batholiths (28°S to 31°S). Geol. Soc. Am. Bull. 104 (8), 999–1014.
Nelson, J., Paradis, S., Christensen, J., Gabites, J., 2002. Canadian Cordilleran Mississippi Valley-type deposits: a case for Devonian-Mississippian back-arc hydrothermal origin. Econ. Geol. 97, 1013–1036.
Núñez, E., 1979. Descripción Geológica de la Hoja 28d, Estación Soitué, Provincia de Mendoza. Serv. Geol. Nac. Bol. 166, 1–67.
Oliva-Urcia, B., Pueyo, E.L., 2007. Rotational basement kinematics deduced from remagnetized cover rocks (Internal Sierras, sothwestern Pyrenees). Tectonics 26. TC4014, 22 pp.
Oliver, J., 1986. Fluids expelled tectonically from orogenic belts: their role in hydrocarbon migration and other geologic phenomena. Geology 14 (2), 99–102.
Padula, E., 1951. Contribución al conocimiento geológico del ambiente de la Cordillera Frontal, Sierra Pintada, San Rafael (Mendoza). Rev. Asoc. Geol. Argent. 6 (1), 5–13.
Ramos, V.A., 1995. Sudamérica: un mosaico de continentes y océanos. Cienc. Hoy 6, 24–29.
Ramos, V.A., 2004. Cuyania, an exotic block to Gondwana: review of a historical success and the present problems. Gondwana Res. 7 (4), 1009–1026.
Ramos, V.A., Dallmeyer, R.D., Vujovich, G., 1998. Time constraints on the Early Palaeozoic docking of the Precordillera, central Argentina. Geol. Soc., Lond 142 (1), 143–158. Special Publications.
Rapalini, A.E., 2012. Paleomagnetic evidence for the origin of the Argentine Precordillera, fifteen years later: what is new, what has changed, what is still valid? Latinmag Lett. 2 (1). LL12–0102Rv, 1-20.
Rapalini, A.E., Tarling, D.H., 1993. Multiple magnetizations in the Cambrian-Ordovician carbonate platform of the Argentine Precordillera and their tectonic implications. Tectonophysics 227 (1–4), 49–62.
Rapalini, A.E., Vilas, J.F., 1991. Tectonic rotations in the Late Palaeozoic continental margin of southern South America determined and dated by palaeomagnetism. Geophys. J. Int. 107 (2), 333–351.
Rapalini, A., Astini, R., 1998. Paleomagnetic confirmation of the Laurentian origin of the Argentine Precordillera. Earth Planet. Sci. Lett. 155 (1–2), 1–14.
Rapalini, A.E., Bordonaro, O., Berquo, T.S., 2000. Paleomagnetic study of Cambrian-Ordovician rocks in the Eastern Precordillera of Argentina: some constraints on the Andean uplift of this block. Tectonophysics 326 (1–2), 173–184.
Rapalini, A.E., Cingolani, C.A., 2004. First Late Ordovician paleomagnetic pole for the Cuyania (Precordillera) terrane of Western Argentina: a microcontinent or a Laurentian plateau. Gondwana Res. 7 (4), 1089–1104.
Rapalini, A.E., Astini, R.A., 2005. La remagnetización sanrafaélica de la Precordillera en el Pérmico: Nuevas evidencias. Rev. Asoc. Geol. Argent. 60 (2), 290–300.
Rocha-Campos, A.C., Basei, M.A., Nutman, A.P., Kleiman, L.E., Varela, R., Llambías, E., Canile, F.M., da Rosa, O., de, C.R., 2011. 30 million years of Permian volcanism recorded in the Choiyoi igneous province (W Argentina) and their source for younger ash fall deposits in the Paraná Basin: SHRIMP U-Pb zircon geochronology evidence. Gondwana Res. 19 (2), 509–523.
Rubinstein, N.A., Ostera, H.A., Mallimacci, H., Carpio, F., 2004. Lead isotopes from Gondwanan polymetallic ore vein deposits, San Rafael Massif, Argentina. J. South Am. Earth Sci. 16 (7), 579–586.
Salmon, E., Edel, J.B., Pique, A., Westphal, M., 1988. Possible origins of Permian remagnetizations in Devonian and Carboniferous limestones from the Moroccan anti-atlas (Tafilalet) and Meseta. Phys. Earth Planet. Inter 52 (3), 339–351.
Schmidt, V., Günther, D., Hirt, A.M., 2006. Magnetic anisotropy of calcite at room-temperature. Tectonophysics 418 (1–2), 63–73.
Sun, W., Jackson, M., Craddock, J.P., 1993. Relationship between remagnetization, magnetic fabric and deformation in Paleozoic carbonates. Tectonophysics 221 (3–4), 361–366.
Symons, D.T.A., Cioppa, M.T., 2000. Crossover plots: a useful method for plotting SIRM data in paleomagnetism. Geophys. Res. Lett. 27 (12), 1779–1782.
Torsvik, T.H., Brinden, J.C., Smethurst, M.A., 2000. Super-IAPD2000. Interactive Analysis of Palaeomagnetic Data. Geological Survey of Norway. Trondheim, Norway.
Thomas, W.A., Tucker, R.D., Astini, R.A., 2000. Rifting of the Argentine Precordillera from Southern Laurentia: Palinspastic Restoration of Basement Provinces. In: Geol. Soc. Am., Abstracts with Programs, vol. 32 p. A-505.
Trindade, R.I.F., D'Agrella-Filho, M.S., Babinski, M., Font, E., Brito Neves, B.B., 2004. Paleomagnetism and geochronology of the Bebedouro cap carbonate: evidence for continental-scale Cambrian remagnetization in the São Francisco craton, Brazil. Precambrian Res. 128 (1–2), 83–103.
Truco, S., Rapalini, A.E., 1996. New evidence of a widespread Permian remagnetizing event in the central Andean zone of Argentina. In: Third International Symposium on Andean Geodynamics, St. Malo, Extended Abstracts, pp. 799–802.
Truco, S.I., 1996. Estudio paleomagnético y geología de la región de Ponón Trehué, Departamento de San Rafael, provincial de Mendoza. Trabajo final de Licenciatura. Universidad de Buenos Aires, 77 pp.
Van der Voo, R., Torsvik, T.H., 2012. The history of remagnetizations of sedimentary rocks: deceptions, developments and discoveries. In: Elmore, R.D., Muxworthy, A.R., Aldana, M.M., Mena, M. (Eds.), Remagnetization and Chemical Alteration of Sedimentary Rocks, Geol. Soc. London, Spec. Publ. 371, pp. 23–53.
Vilas, J.F., Valencio, D.A., 1978. Palaeomagnetism and K-Ar age of the Upper Ordovician Alcaparrosa Formation, Argentina. Geophys. J. Int. 55 (1), 143–154.
Weil, A.B., Van der Voo, R., 2002. Insights into the mechanism for orogen-related carbonate remagnetization from growth of authigenic Fe-oxide: a scanning electron microscopy and rock magnetic study of Devonian carbonates from northern Spain. J. Geophys. Res. Earth 107 (B4), 14.
Zegers, T.E., Dekkers, M.J., Bailly, S., 2003. Late Carboniferous to Permian remagnetization of Devonian limestones in the Ardennes: role of temperature, fluids, and deformation. J. Geophys. Res. 108 (B7), 19.
Zijderveld, J.D.A., 1967. A.C. desmagnetization of rocks: analysis of results. In: Collinson, D.W., Creer, K.M., Runcorn, S.K. (Eds.), Methods in Palaeomagnetism. Elsevier, Amsterdam, pp. 254–286.
Zwing, A., Matzka, J., Bachtadse, V., Soffel, H.C., 2005. Rock magnetic properties of remagnetized Palaeozoic clastic and carbonate rocks from the NE Rhenish massif, Germany. Geophys. J. Int. 160 (2), 477–486.